Donor-Substituted Cyanoethynylethenes: π-Conjugation and Band-Gap Tuning in Strong Charge-Transfer Chromophores

Nicolle N. P. Moonen,[a] William C. Pomerantz,[a] Robin Gist,[a] Corinne Boudon,[b] Jean-Paul Gisselbrecht,[b] Tsuyoshi Kawai,[c] Atsushi Kishioka,[c] Maurice Gross,[b] Masahiro Irie,[c] and François Diederich*[a]

Abstract: An extensive series of silyl-protected cyanoethynylethenes (CEEs) and *N*,*N*-dimethylanilino donor-substituted CEEs have been synthesized. More extended chromophores were constructed by selective silyl deprotection and subsequent oxidative acetylenic coupling. The strong electron-accepting nature of the CEEs was revealed by a combination of ^{13}C NMR spectroscopic and electrochemistry measurements. Donor-substituted CEEs display strong intramolecular charge-transfer (CT) character, resulting in intense, bathochromically shifted CT bands in the UV/Vis spectrum. Their structural diversity establishes them as suitable models for the study of π-conjugation and band gap tuning in strong charge-transfer chromophores. The extent of π-conjugation in the donor-substituted CEEs was investigated by a combination of ground-state techniques, such as X-ray crystallography, electrochemistry, B3LYP calculations, and NMR spectroscopy. The comparison of these ground-state results with the features observed in the UV/Vis spectra reveals that—contrary to expectations—more extensive π-conjugation can lead to larger band gaps in molecules with strong donor and acceptor moieties.

Keywords: alkynes · charge transfer · conjugation · electrochemistry · two-photon absorption

Introduction

Tetraethynylethene (3,4-diethynylhex-3-ene-1,5-diyne, TEE, $C_{10}H_4$) and its silylated derivatives such as **1**[1] are versatile building blocks for the synthesis of large one- and two-dimensional scaffolds,[2] such as poly(triacetylene) oligomers, expanded radialenes, dehydroannulenes, and most recently radiaannulenes.[3] Conjugation of TEEs with the *N*,*N*-dimethylanilino (DMA) donor (D) and *p*-nitrophenyl acceptor (A) groups resulted in a new class of intramolecular charge-transfer (CT) chromophores,[4] which showed very good second- and third-order nonlinear optical (NLO) properties. By studying a variety of donor–acceptor-substituted TEEs, structure–property relationships for the first[5] and second hyperpolarizability[6] (β and γ) were established.

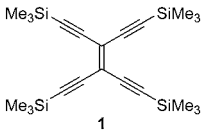

1

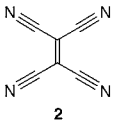

2

Tetracyanoethene (TCNE, **2**) is isoelectronic with TEE and one of the strongest organic electron acceptors known. TCNE has been widely used for the formation of intermolecular charge-transfer salts, and its chemical reactivity towards nucleophiles and in cycloadditions has been extensively studied.[7]

The family of hybrid compounds between TEE and TCNE, the cyanoethynylethenes (CEEs), was until recently rather unexplored. Miller and co-workers,[8] and later Hopf et al.[9] reported the synthesis of some geminal dicyanodiethynylethenes [2-(1-ethynylprop-2-ynylidene)malononitriles]. The latter authors demonstrated the enhanced reactivity of their C≡C triple bonds in Diels–Alder reactions[9a]

[a] Dr. N. N. P. Moonen, W. C. Pomerantz, R. Gist, Prof. Dr. F. Diederich
Laboratorium für Organische Chemie
ETH-Hönggerberg, HCI, 8093 Zürich (Switzerland)
Fax: (+41) 1-632-1109
E-mail: diederich@org.chem.ethz.ch

[b] Dr. C. Boudon, Dr. J.-P. Gisselbrecht, Prof. Dr. M. Gross
Laboratoire d'Electrochimie et de Chimie Physique du Corps Solide
UMR 7512, C.N.R.S, Université Louis Pasteur
4, rue Blaise Pascal, 67000 Strasbourg (France)

[c] T. Kawai, A. Kishioka, Prof. M. Irie
Department of Chemistry and Biochemistry
Graduate School of Engineering, Kyushu University
Hakozaki 6–10–1, Higashiku, Fukuoka 812–8581 (Japan)

Supporting information for this article is available on the WWW under http://www.chemeurj.org/ or from the author.

 DOI: 10.1002/chem.200500082

and in a [2+2] cycloaddition with tetrathiafulvalene (TTF), followed by ring opening.[9b] A small series of aryl-substituted tricyanomonoethynylethenes was reported by Ukhin and co-workers,[10] and by Heinze, Dulog, and co-workers.[11]

CEEs combine the scaffolding capacity of TEEs with the electron-accepting properties of TCNE, thereby providing a versatile class of modular building blocks for the construction of novel conjugated π-systems. In addition, introduction of electron donors should result in the formation of strong intramolecular charge-transfer (CT) chromophores. Here, we report the synthesis of the monomeric and dimeric, silyl-protected CEEs **3**–**11**[12] and the *N*,*N*-dimethylanilino (DMA) donor-substituted derivatives **12**–**24**.[13] We demonstrate the use of CEEs as modules in acetylenic scaffolding and characterize their electronic properties in a systematic study. In particular, X-ray crystallography, electrochemistry, density functional calculations, and NMR spectroscopy are applied to analyze the extent of π-electron conjugation and the efficiency of particular donor–acceptor conjugation paths in these novel chromophores; physical quantities that greatly influence properties such as optical nonlinearities.[6a,14]

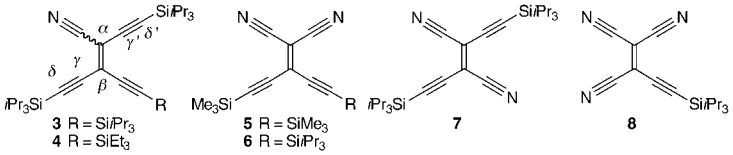

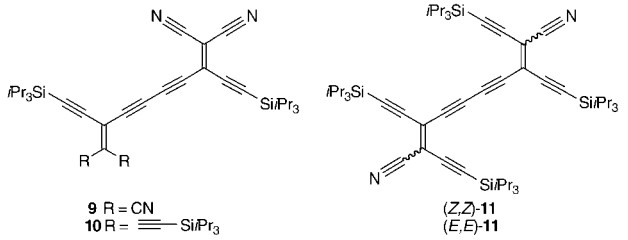

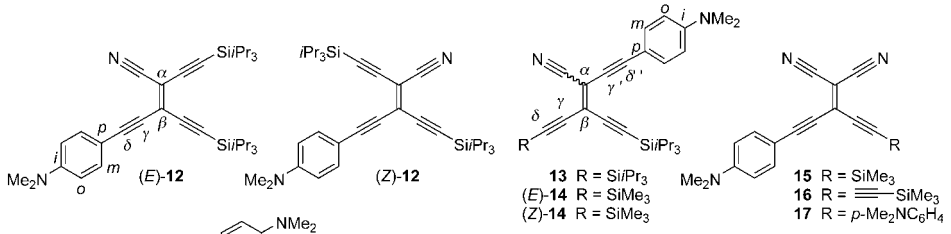

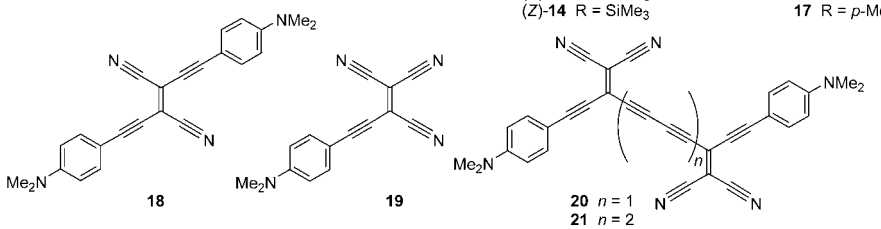

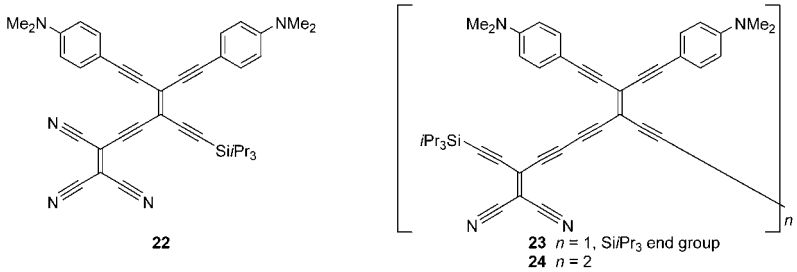

Results and Discussion

Synthesis of monomeric cyanoethynylethenes: Monocyanotriethynylethenes were prepared in a Knoevenagel reaction between penta-1,4-diyne-3-ones **25**–**27**[15–17] and 4-(triisopropylsilyl)but-3-ynenitrile, obtained by cyanation of (3-bromopropynyl)triisopropylsilane[18] with CuCN in DMF.[19] Thus, the reaction of Si*i*Pr$_3$-protected **27** in the presence of Hünig's base (8 h, reflux) provided monocyanotriethynylethene **3** in an excellent yield of 97% (Scheme 1). With the sterically less encumbered, SiEt$_3$-protected ketone **26**,[16] the conversion was finished within a minute at 20°C, yielding **4**, the isomers of which could not be separated, besides relatively large amounts of the monodeprotected isomers (*Z*)-**28** and (*E*)-**28** that were separable by chromatography. The isomeric mixture **4** was readily transformed into (*Z*)-**28** and (*E*)-**28** by protodesilylation (K_2CO_3, THF/MeOH).

Hopf and Kreutzer[9a] had reported a high-yielding synthesis of the SiMe$_3$-protected geminal dicyanodiethynylethene **5**[8] by reacting SiMe$_3$-protected ketone **25** with malononitrile using Al_2O_3 as catalyst.[20] This method was also applied to afford differentially protected CEE **6** in a good yield of 85%. All attempts to monodeprotect **6** under formation of **29** failed under standard conditions (nBu$_4$NF in THF at −78°C, or K_2CO_3 or borax in THF/MeOH), and only decomposition was observed. Fortunately, yields between 60% and 95% (thin-layer chromatography (TLC)) of free alkyne **29** were obtained by simply dissolving **6** in MeOH/THF (5:1) in the absence of any base. This facile deprotection demonstrates in an impressive way the high electrophilicity of the Si center due to the strongly electron-withdrawing nature of the appended CEE chromophore.

Remarkably and, to the best of our knowledge, without precedence in the chemistry of silylated alkynes, the deprotection of **6** was found to be reversible. Upon changing from MeOH/THF to THF, deprotected CEE **29** had reverted back to SiMe$_3$-protected **6**. Monitoring

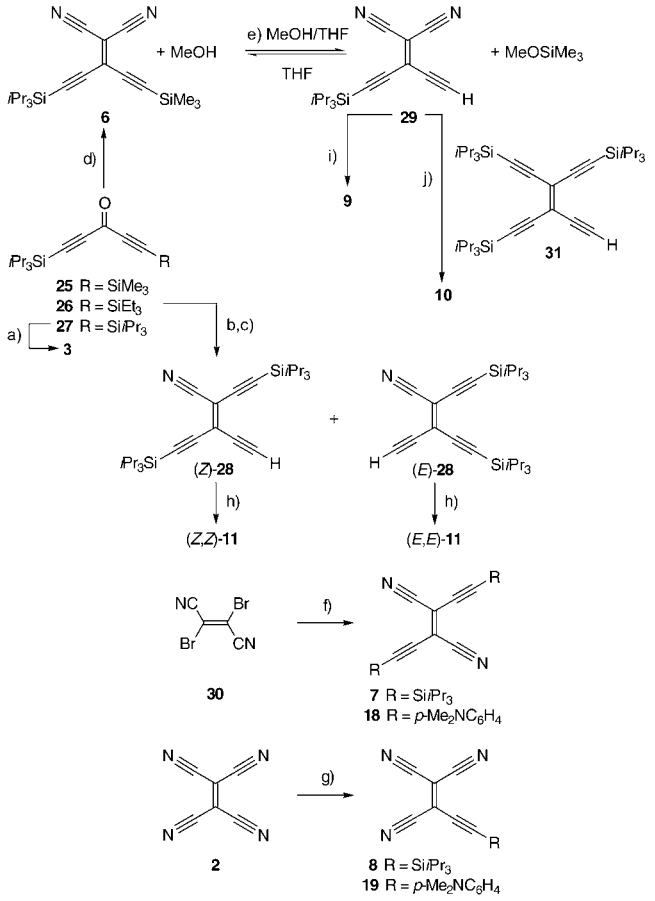

Scheme 1. Synthesis of monomeric and dimeric CEEs. a) iPr$_3$SiC≡C-CH$_2$CN, iPr$_2$EtN, EtOH, Δ; 97%; b) iPr$_3$SiC≡CCH$_2$CN, iPr$_2$EtN, EtOH, 20°C; **4** (47%), (*Z*)-**28** (27%), (*E*)-**28** (15%); c) K_2CO_3, THF/MeOH 1:1, 20°C; (*Z*)-**28** (46%), (*E*)-**28** (29%); d) $CH_2(CN)_2$, Al_2O_3 (act. II-III), CH_2Cl_2, 40°C; 85%; e) THF/MeOH 1:5; 20°C; f) iPr$_3$SiC≡CH or *p*-Me$_2$NC$_6$H$_4$C≡CH, [PdCl$_2$(PPh$_3$)$_2$], iPr$_2$NH, CuI, THF, 20°C; **7** (30%), **18** (52%); g) iPr$_3$SiC≡CLi, CuBr, THF, 50°C; **8** (33%) or *p*-Me$_2$NC$_6$H$_4$-C≡CH, CuOAc, THF, 50°C; **19** (29%); h) CuCl, TMEDA, CH_2Cl_2, 20°C; (*Z*,*Z*)-**11** (91%), (*E*,*E*)-**11** (85%); i) Cu(OAc)$_2$, CH_2Cl_2, 20°C; 22% (from **6**); j) **31** (2.5 equiv), Cu(OAc)$_2$, CH_2Cl_2, 20°C; 27% (from **6**). TMEDA = *N*,*N*,*N*′,*N*′-tetramethylethylenediamine.

the slow addition of MeOH to a solution of **6** in THF revealed that the deprotection started to proceed at a THF/MeOH ratio of 1:1.

The preparation of the *trans*-dicyanodiethynylethene **7** started from dibromofumaronitrile (**30**) obtained by bromination of dicyanoacetylene (Scheme 1).[21] Cross-coupling of **30** with iPr$_3$Si–C≡CH under standard Sonogashira conditions (CuI, [PdCl$_2$(PPh$_3$)$_2$], Et$_3$N)[22] yielded only a mixture of uncharacterized products. On the other hand, the use of the more hindered base iPr$_2$NH resulted in a 30% yield of **7**, besides some unidentified products. Changing to the even more hindered Hünig's base lowered the yield to 19%, and more by-products were observed.

Dulog et al. reported the synthesis of several aryl-substituted tricyanomonoethynylethenes[11] from TCNE and copper(I) arylacetylides, prepared from the corresponding acetylenes with CuOAc. The yield of this nucleophilic addition–elimination reaction increased with increasing electron-donating character of the aryl ring. Attempts to synthesize the SiiPr$_3$-protected CEE **8** by this method failed. Presumably, the copper acetylide was not formed in the reaction of iPr$_3$Si–C≡CH with CuOAc. However, when the copper acetylide was generated by transmetalation of iPr$_3$Si–C≡C–Li with CuBr[23] and subsequently reacted with TCNE, CEE **8** was isolated in a yield of 33% (Scheme 1).

Synthesis of dimeric cyanoethynylethenes: The dimeric CEEs (*Z*,*Z*)-**11** and (*E*,*E*)-**11** were prepared in good yields by homocoupling of monodeprotected monocyanotriethynylethenes (*Z*)-**28** and (*E*)-**28**, respectively, under Hay conditions (CuCl, TMEDA, CH_2Cl_2, air, Scheme 1).[24] Dimer (*E*,*E*)-**11** was found to be rather unstable and was converted under influence of light or heat into the more stable (*Z*,*Z*) isomer. The initial, NMR-based configurational assignment of isomers (*Z*)-**28** and (*E*)-**28** was confirmed by an X-ray crystal structure analysis of (*Z*,*Z*)-**11**.[12]

Attempted oxidative homocoupling[25] of free alkyne **29** to give **9** under Hay[24] or Eglinton (Cu(OAc)$_2$, MeOH, pyridine, O_2) conditions[26] led to immediate decomposition of the starting material. This was also the result of coupling attempts with Cu(OAc)$_2$ and various nitrogen bases such as 2,6-lutidine, aniline, 2,6-dimethylaniline, or imidazole in CH_2Cl_2. On the other hand, a yield of 22% of **9** was obtained with Cu(OAc)$_2$ in CH_2Cl_2 in the absence of any nitrogen bases to avoid nucleophilic attack on the CEE. The acidifying effect of the electron-withdrawing cyano groups in **29** was evidently large enough to achieve the oxidative coupling in the absence of any base. Under similar base-free conditions, the mixed TEE/CEE dimer **10** was prepared by reacting **29** with 2.5 equivalents of **31**.[15]

All silyl-protected monomeric and dimeric CEEs are air-stable compounds, but with increasing electron-accepting power, the sensitivity towards nucleophiles increases. For example, (*E*)- and (*Z*)-**28** with one cyano group are stable under Hay coupling conditions, whereas dinitrile **29** decomposes instantaneously under these conditions. CEE **8**, containing three cyano groups, is readily prone to nucleophilic attack and decomposes even slowly in MeCN.

Synthesis of donor-substituted CEEs: In contrast to the high reactivity of CEE **8**, the DMA donor-substituted tricyanoethynylethene **19**, prepared according to Dulog et al.[11] by reacting TNCE with the copper(I) acetylide formed from *N*,*N*-dimethyl-4-ethynylaniline (Scheme 1), features high stability. Solutions of **19** are bright blue, and the shiny metallic solid can be sublimed undecomposed at 100°C/0.1 mbar. A pronounced stabilization of CEEs upon introduction of DMA donor moieties is a general feature and can be readily explained by intramolecular charge-transfer stabilization, which reduces the electrophilicity of the electron-deficient CEE core. A similar stabilization has also been observed upon introduction of DMA donor groups into the C(sp)-rich, electron-deficient all-carbon cores of perethynylated dehydroannulenes and radiaannulenes.[3]

The *trans*-disubstituted CEE **18** with two DMA donor moieties was readily prepared by Sonogashira cross-coupling between dibromofumaronitrile **30** and *N*,*N*-dimethyl-4-ethynylaniline (Scheme 1). CEE **18** is a stable, metallic solid and sublimes undecomposed at 160 °C/0.1 mbar.

The synthesis of several DMA-substituted CEEs started with the addition of lithiated *N*,*N*-dimethyl-4-ethynylaniline to the protected propargyl aldehydes **32** and **33** or twofold addition to ethyl formate, yielding the rather unstable alcohols **34**–**36**, respectively (Scheme 2).[27–29] Subsequent oxidation with MnO_2 gave ketones **37**–**39**.[28,29] Knoevenagel reaction of **37** with 4-(triisopropylsilyl)but-3-ynenitrile in the presence of Hünig's base provided a mixture of (*E*)- and (*Z*)-**12**, which could be separated by column chromatography in the dark. The configuration of the two isomers was unambiguously assigned with the help of one-dimensional NOE ^{1}H NMR experiments. The two Si*i*Pr$_3$ groups within one molecule showed separate signals in the ^{1}H NMR spectrum and could be selectively irradiated. For (*Z*)-**12**, both irradiations resulted in an NOE transfer to the proton *meta* to the Me_2N group of the aryl ring at $\delta = 7.4$ ppm. In the case of (*E*)-**12**, only one of the two irradiations resulted in a small NOE effect. This assignment also agrees with the observation that (*Z*)-**12** is a solid and (*E*)-**12** an oil; two Si*i*Pr$_3$ groups in *cis* positions often prevent good packing of TEEs and CEEs into a solid.

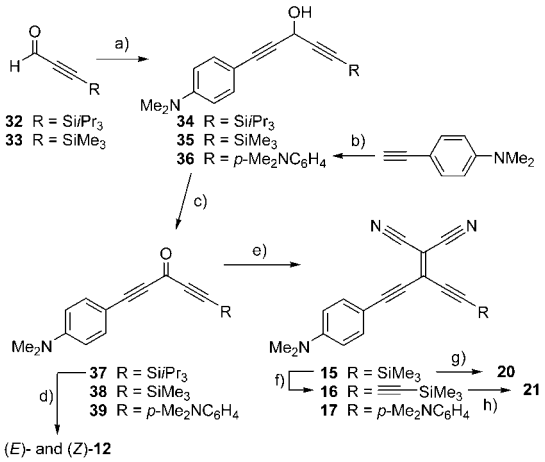

Scheme 2. Synthesis of donor-substituted CEEs. a) *p*-$Me_2NC_6H_4C{\equiv}CLi$, THF, −15 °C→0 °C; **34** (60 %), **35** (80 %); b) *n*BuLi, ethyl formate, THF, −15 °C→0 °C; **36** (57 %); c) MnO_2, CH_2Cl_2, or EtO_2, 20 °C; **37** (80 %), **38** (84 %), **39** (81 %); d) *i*$Pr_3SiC{\equiv}CCH_2CN$, *i*Pr_2EtN, EtOH, 20 °C; (*Z*)-**12** (30 %), (*E*)-**12** (50 %); e) $CH_2(CN)_2$, Al_2O_3 (act. II-III), CH_2Cl_2, Δ; **15** (77 %), **17** (65 %); f) THF/MeOH 1:1, then $H{-}C{\equiv}C{-}SiMe_3$, CuCl, TMEDA, CH_2Cl_2, air, 20 °C; 24 %; g) THF/MeOH 1:1, then CuCl, TMEDA, CH_2Cl_2, air, 20 °C; 19 %; h) THF/MeOH 1:1, then $Cu(OAc)_2$, THF, air, 20 °C; 79 %.

The Knoevenagel reaction of $SiMe_3$-protected ketone **38** with malononitrile, catalyzed by Al_2O_3, gave **15** in a yield of 77 % (Scheme 2). The same transformation of the less reactive ketone **39** with malononitrile afforded **17** in a yield of only 65 %. The $SiMe_3$ protecting group in CEE **15** was removed under mild conditions in MeOH/THF (see above), and slow addition of Hay catalyst to deprotected **15** in CH_2Cl_2 afforded dimer **20**. Heterocoupling of deprotected **15** with $Me_3Si{-}C{\equiv}CH$ gave **16** in yields up to 24 %. Deprotection of **16** with MeOH/THF and homocoupling in the presence of $Cu(OAc)_2$ in THF provided the octa-1,3,5,7-tetraynediyl-spaced "dimeric" CEE **21** in a high yield of 79 %.

CEEs **13** and (*E*)/(*Z*)-**14** with geminal donor–acceptor functionalization were obtained in excellent yields by Sonogashira cross-coupling between *N*,*N*-dimethyl-4-ethynylaniline and vinyl chlorides **40** or **41**, respectively (Scheme 3).

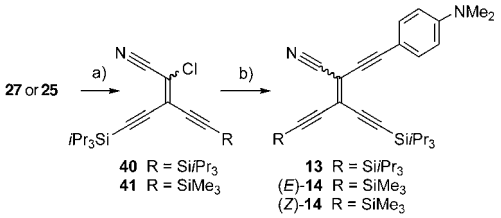

Scheme 3. Synthesis of CEEs with geminal donor-acceptor alignment. a) Diethyl 1-chloro-1-cyanomethylphosphonate, *n*BuLi, THF, −78 °C, then **27** or **25**; **40** (92 %), **41** (86 %); b) *p*-$Me_2NC_6H_4C{\equiv}CH$, [$PdCl_2(PPh_3)_2$], CuI, *i*Pr_2NH, THF, 20 °C; **13** (94 %), (*E*)-**14** (58 %) and (*Z*)-**14** (42 %).

Compounds **40** and **41** were prepared by deprotonation of diethyl 1-chloro-1-cyanomethylphosphonate[30] with *n*BuLi, followed by reaction with ketones **27** or **25**, respectively. The configuration of (*E*)- and (*Z*)-**14** was again assigned by one-dimensional NOE ^{1}H NMR spectroscopy. Upon irradiation of the Si*i*Pr$_3$ protons of (*E*)-**14** or the $SiMe_3$ protons of (*Z*)-**14**, an NOE transfer to the *meta* protons of the aniline ring

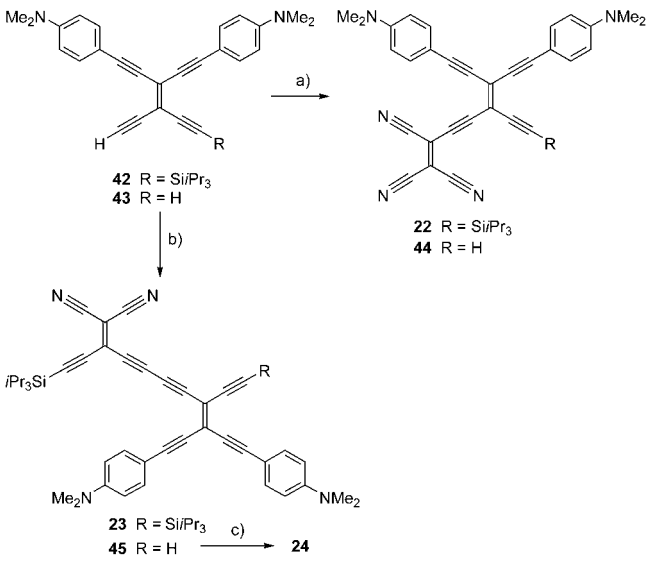

Scheme 4. Synthesis of CEEs **22**–**24**: a) CuOAc, THF/MeCN 6:1, TCNE, 50 °C; **22** (21 %), **44** (7 %); b) CEE **6**, $Cu(OAc)_2$, MeOH/THF 1:1 or 2:3, 20 °C; **23** (13 %), **45** (18 %); c) CuCl, TMEDA, air, CH_2Cl_2, 20 °C; 70 %.

was observed. No NOE was detected upon irradiation of the second silyl protecting group in the molecules.

Another series of extended donor-acceptor chromophores was obtained starting from TEEs **42** and **43**[31] (Scheme 4). Nucleophilic substitution of TCNE by the copper(I) acetylide formed from **42** afforded CEE **22** with two DMA donor and three cyano acceptor groups in 21% yield (Scheme 4). On the other hand, efforts to react the bis(copper(I) acetylide) of **43** with two TCNE molecules were only partially successful and afforded the monosubstitution product **44** in low yield (≈7%).

The oxidative heterocoupling of TEE **42** with CEE **29** (Scheme 1) in CH_2Cl_2 in the presence of $Cu(OAc)_2$ was found to be very slow, with heterodimer **23** being formed in only 9% yield over a period two weeks (Scheme 4). When CEE **6** was deprotected in situ to **29** in THF/MeOH 1:1 and reacted with **42** in the presence of $Cu(OAc)_2$, **23** was isolated in 13% yield after 6–8 h. Finally, the extended chromophore **24** with four donor and four acceptor residues was obtained by oxidative heterocoupling of bisdeprotected TEE **43** with an excess of **29** to give **45** (18% yield), followed by homocoupling (CuCl, TMEDA, air, CH_2Cl_2, 70% yield).

NMR investigations: We analyzed the ^{13}C NMR spectra of the CEEs in $CDCl_3$ in order to identify possible effects of π-electron conjugation on the chemical shifts. The data for monomeric CEEs are listed in Table 1.

The chemical shift of C atoms strongly depends on hybridization and the electron density at the nucleus. The higher the electron density, the more shielding occurs and an upfield shift will be observed.[32] Hall and co-workers investigated the chemical shifts of olefins with CN substituents.[33] An upfield shift was observed for the C atoms of the CN groups with an increasing number of such groups connected to the double bond. This upfield shift is also observed upon going from **3** (1 CN), through **7** (2 CN) and **8** (3 CN), to TCNE (**2**). Remarkable is the larger upfield shift in going from **3** to geminally substituted **5** ($\Delta\delta = -3.44$ ppm) compared to the change from **3** to *trans*-substituted **7** ($\Delta\delta = -2.23$ ppm). Similarly, Hall and co-workers reported an additivity increment for a geminal substituent of −3.93 ppm and a smaller one of −1.60 ppm for a *trans* substituent.

The chemical shift of the alkyne γ-C atom (and γ′-C atom if applicable; for atom labeling, see structural formulae of compounds **3** and **4** above) around $\delta = 99$ ppm is weakly dependent on the substituents at the double bond (maximum $\Delta\delta = 3.7$ ppm). In contrast, the chemical shift of the alkyne δ-C (and δ′-C) atom is more sensitive to structural variation with a maximum difference in chemical shift of 16.9 ppm (**1** versus **8**). The difference in chemical shift between the γ- and δ-C atoms ($\Delta\delta_{\delta-\gamma}$) in a single compound increases with the number of CN groups. In TEE **1** (0 CN), the difference is only 4.3 ppm, whereas in **8** (3 CN) the difference increases to 25.44 ppm. This shift difference can be seen, together with the chemical shift for the CN carbon atom, as a measure for the acceptor strength of the CEEs. The lower the value of δ_{CN} and the larger $\Delta\delta_{\delta-\gamma}$, the higher the acceptor strength of the molecule. Geminal CEE **6** was indeed identified as a better electron acceptor than *trans*-substituted CEE **7** in electrochemical measurements (vide infra).

The α-, γ- (and γ′-), and *para*-C atoms (for the labeling, see structural formulae of compounds **12–14** above) of the donor-substituted CEEs could not be unambiguously assigned in the ^{13}C NMR spectra, since their chemical shift values were too similar. A minimum value is indicated for the γ-C (and γ′-C) atoms in Table 2. The extended structures **20–24** were not taken into consideration, since the spectral assignment was too complicated.

As for the parent CEEs (vide supra), an upfield shift is observed for the CN carbon atom resonance with increasing number of CN residues. The introduction of the DMA donor groups results in a downfield shift of δ_{CN} (relative to the parent CEEs). This downfield shift is a measure for the effectiveness of donor–acceptor (D–A) conjugation in the ground state. For cross-conjugated **13**, a downfield shift $\Delta\delta_{CN}$ of only 0.2 ppm is observed (comparison with **3**). The linearly conjugated (*E*)-**12** and (*Z*)-**12**, on the other hand, show downfield shifts $\Delta\delta_{CN} = 1.0$ and 0.7 ppm, respectively. From these results, it can be concluded that the *cis* D–A conjugation path in (*E*)-**12** is more effective than the *trans* D–A path in (*Z*)-**12**. Also, linear conjugation is much more efficient than cross-conjugation.

Table 1. ^{13}C NMR chemical shifts (75 MHz, $CDCl_3$) of representative CEEs and reference compounds.[a]

	Number of CN groups	δ_{CN}	$\delta_{C\equiv C,\gamma,\gamma'}$	$\delta_{C\equiv C,\delta,\delta'}$
1[11b]	0	–	101.0	105.3
3	1	115.10	98.99	106.74
			101.72	107.60
			101.73	108.62
7	2	112.87	97.27	114.42[b]
5[16]	2	111.66	97.53	117.87
8	3	109.59	96.77	122.21
		109.74		
		110.66		
2[30]	4	107.84	–	–

[a] Chemical shifts (δ) are indicated in ppm downfield from $SiMe_4$, using the residual signal of $CHCl_3$ as an internal reference. [b] Assignment not certain, value possibly 114.97.

Table 2. ^{13}C NMR chemical shifts [in ppm; 75 MHz, $CDCl_3$] of donor-substituted CEEs.

	δ_{CN}	$\delta_{C\equiv C,\delta,\delta'}$	$\delta_{C\equiv C,\gamma,\gamma'}$	δ_{ipso}	δ_{ortho}	δ_{meta}
(*E*)-**12**	116.08	86.88	≥99.68	151.14	111.49	133.95
(*Z*)-**12**	115.81	86.56	≥99.76	151.06	111.40	133.79
13	115.34	83.52	≥102.09	150.95	111.46	133.37
15	112.86	88.56	89.82	152.28	111.55	135.37
	113.02					
17	112.52	84.58	87.58	151.98	111.53	135.03
18	114.08	84.37	≥106.47	151.42	111.58	133.93
19	111.36	91.00	91.06	153.41	112.10	136.38
	111.40					
	111.55					

Whereas the chemical shift difference between the alkyne γ- (and γ′) and δ- (and δ′-) carbon atoms ($\Delta\delta_{\delta-\gamma}$) increases with the acceptor strength (vide supra), the introduction of a DMA donor group reduces this difference. The value of $\Delta\delta_{\delta-\gamma}$ becomes smaller with increasing intramolecular CT from the donor to the acceptor moiety. A decrease in $\Delta\delta_{\delta-\gamma}$ from $\geq$12.8 to 1.3 ppm, and to 0.06 ppm is observed upon changing from (*E*)-**12** (1 CN), to **15** (2 CN), and to **19** (3 CN), respectively.

The downfield shift of the aryl C-atoms and the protons in *meta* positions relative to the DMA group (Tables 2 and 3, respectively) can also be considered as a measure for the efficiency of donor–acceptor conjugation. The downfield shifts decrease from (*E*)-**12**, to (*Z*)-**12**, and to geminal **13**, suggesting a more effective conjugation pathway for the linearly D–A-substituted chromophores. The increase in the number of CN groups per DMA donor moiety upon changing from (*E*)-**12** (1 CN), to **15** (2 CN), and to **19** (3 CN) also produces a downfield shift evidencing enhanced D–A conjugation.

Table 3. ^{1}H NMR chemical shifts [in ppm; 300 MHz, $CDCl_3$] of donor-substituted CEEs.

	δ_{ortho}	δ_{meta}	Compound	δ_{ortho}	δ_{meta}
(*E*)-**12**	6.63	7.42	**19**	6.70	7.54
(*Z*)-**12**	6.63	7.37	**20**	6.67	7.55
13	6.63	7.36	**21**	6.67	7.52
15	6.65	7.51	**22**	6.65, 6.67	7.47, 7.54
16	6.65	7.50	**23**	6.62, 6.68	7.43, 7.46
17	6.65	7.53	**24**	6.58, 6.73	7.44, 7.50
18	6.65	7.46			

From the NMR spectral data in Table 2, the efficiency of D–A conjugation, that is, the amount of CT can be determined as **19** > **15** > **17** > **18** > (*E*)-**12** > (Z)-**12** > **13**.

Interestingly, the ^{1}H NMR spectra of the extended chromophores **22** and **24** exhibit a strong differentiation between the DMA groups within each molecule (Table 3). The upfield resonance indicates weaker participation in D–A conjugation pathways, the downfield one stronger conjugation.

X-ray structures and bond-length alternation: All donor-substituted CEEs except (*E*)-**12** are solids. The monomeric chromophores are shiny metallic substances and the larger structures black amorphous materials. The crystal structures of **18** and **19** are shown in Figure 1 (for details, see reference [13]).

Bond-length alternation in the DMA moiety can be expressed by the quinoid character (δr) of the aryl ring [Eq. (1)].[34] The quinoid character is a good indication for the amount of CT from the DMA donor to the CEE acceptor moiety in the ground state.

$$\delta r = [(a-b) + (c-b)]/2 \approx [(a'-b') + (c'-b')]/2 \quad (1)$$

In benzene, the δr value equals 0 and values between 0.08 and 0.10 are found in fully quinoid rings (see Figure 1 for the definition of bond lengths *a*, *a*′, *b*, *b*′, *c*, and *c*′). Calculated from the X-ray crystal structures (Figure 1), CEE **18** exhibits a δr of 0.033 and **19** has a value of 0.037. The δr values for DMA rings in donor–acceptor substituted TEEs,[4] calculated from several X-ray structures, generally do not exceed 0.025. This demonstrates the enhanced intramolecular CT in donor-substituted CEEs relative to the TEEs.

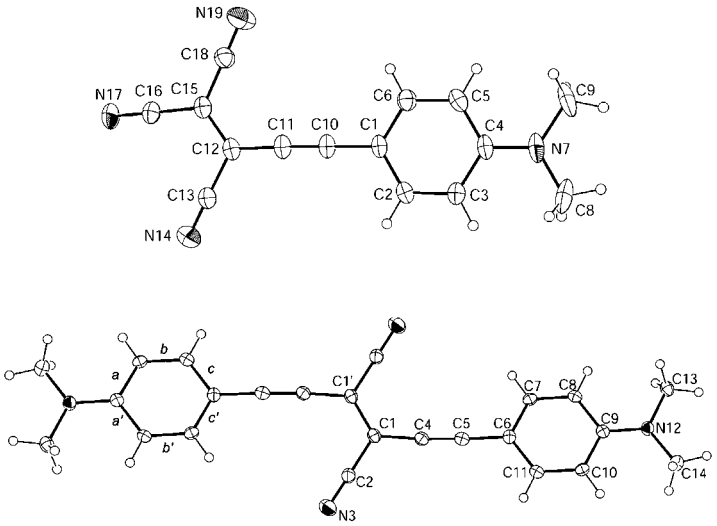

Figure 1. Top: ORTEP representation of **19** with vibrational ellipsoids obtained at 243 K and shown at the 30% probability level. Selected bond lengths [Å]: C1–C2 1.392(2), C1–C6 1.401(2), C2–C3 1.366(2), C3–C4 1.415(2), C4–C5 1.410(3), C4–N7 1.356(2), C5–C6 1.370(2), C10–C11 1.209(2), C1–C10 1.410(2), C11–C12 1.394(2), C12–C15 1.365(3), C15–C16 1.432(2), C16–N17 1.139(2). Bottom: ORTEP representation of **18** with vibrational ellipsoids obtained at 120 K and shown at the 30% probability level. Selected bond lengths [Å]: C1–C1′ 1.372(4), C1–C2 1.441(3), C2–N3 1.146(3), C1–C4 1.417(3), C4–C5 1.207(3), C5–C6 1.422(3), C6–C(7) 1.397(3), C7–C8 1.370(3), C8–C9 1.410(3), C6–C11 1.401(3), C10–C11 1.374(3), C9–C10 1.411(3), C9–N12 1.368(2).

The δr values calculated on the B3LYP/6–31G** level of theory[35] for **18** (0.0315) and **19** (0.0382) are in good agreement with those determined from the X-ray crystal structure data. The δr values of the monomeric donor-substituted CEEs were calculated (Table 4) and suggested a higher amount of CT in the ground state for *cis* D–A-substituted (*E*)-**12** than for *trans* D–A-substituted (*Z*)-**12** and geminally substituted **13** (δr = 0.0318, 0.0314, and 0.0309, respectively). The comparison of constitutional isomers **17** and **18** shows two *cis* and two *trans* D–A pathways for **17**, and two gemi-

Table 4. Quinoid character of monomeric donor-substituted CEEs.

	Calculated δr (B3LYP/6–31G**)	Experimental δr (X-ray)
(*E*)-**12**	0.0318	–
(*Z*)-**12**	0.0314	–
13	0.0309	–
17	0.0320	–
18	0.0315	0.033
19	0.0382	0.037

nal and two *cis* D–A pathways for **18**. Considering that cross-conjugation is less effective than linear conjugation, a larger δr is expected and indeed calculated for **17**. The largest amount of conjugation is found for **19**.

The calculations support the order of efficient D–A conjugation in these molecules as found by the NMR studies (vide supra), being **19** > **17** > **18** > (*E*)-**12** > (Z)-**12** > **13**.

Electrochemistry: The redox properties of the CEEs were studied by using cyclic voltammetry (CV) and rotating disk voltammetry (RDV) in CH_2Cl_2 with nBu$_4$NPF$_6$ (0.1 M) as the supporting electrolyte. The redox potentials versus Fc^+/Fc (ferricinium/ferrocene couple) are listed in Table 5 together with the values for TEEs **1** and **46**,[36] and TCNE (**2**).[37]

Table 5. Cyclic voltammetry data of silyl-protected TEEs and CEEs in CH_2Cl_2 (+0.1 M nBu$_4$NPF$_6$).[a] For an overview of the compounds, see structural formulae in text.

	Cyclic voltammetry			Rotating disk voltammetry	
	E^o [V][b]	ΔE_p [mV][c]	E_p [V][d]	$E_{1/2}$ [V][e]	Slope [mV][f]
1[g]	−1.96	320[h]		−2.02	60
				−2.50	80
				−2.74	160
3	−1.58	90		−1.60	65
			−2.34	−2.35	80
7	−1.25	100		−1.38	60
			−2.05		
6	−1.15	70			
			−1.95		
8	−0.72	85		−0.72	60
			−1.69	−1.70[i]	
2[j]	−0.32				
	−1.35				
46[g]	−1.52	80[h]		−1.52	70
	−1.89	70[h]		−1.88	60
			−2.90	−2.74	110
(*Z*,*Z*)-**11**	−1.07	75		−1.10	60
	−1.37	75		−1.39	60
(*E*,*E*)-**11**	−1.06	60			
	−1.36	60			
10	−0.90	80		−0.90	70
	−1.44	70		−1.48	75
9	−0.57	90		−0.59	62
	−0.84	90		−0.89	60
			−2.24		

[a] Potentials versus the ferricinium/ferrocene couple. Working electrode: glassy carbon electrode; counter electrode: Pt; reference electrode: Ag/AgCl. [b] $E^o = (E_{pc}+E_{pa})/2$, where E_{pc} and E_{pa} correspond to the cathodic and anodic peak potentials, respectively. All reductions are one-electron transfers. [c] $\Delta E_p = E_{ox} - E_{red}$, in which subscripts ox and red refer to the conjugated oxidation and reduction steps, respectively. [d] E_p = Irreversible peak potential at $v = 0.1\ V\,s^{-1}$. [e] $E_{1/2}$ = Half-wave potential. [f] Slope = Slope of the linearized plot of E versus $\log[I/(I_{lim}-I)]$. I_{lim} is the limiting current and I the current. [g] Solvent: THF; working electrode: Hg.[36] [h] Scan rate $v = 10\ V\,s^{-1}$. [i] Small amplitude wave. [j] Quasi reversible electron transfers.[37]

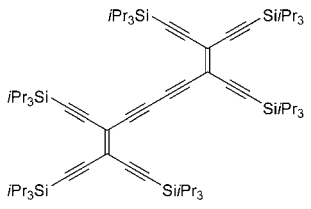

46

All monomeric CEEs show a reversible one-electron reduction step, followed by a second irreversible step. The introduction of additional CN groups (from **1** (0 CN), to **3** (1 CN), to **7** (2 CN), to **8** (3 CN), and TCNE (**2**; 4 CN)) results in an anodic shift of the first reduction potential.[38] On the basis of the first reduction potentials for the monomeric CEEs, the increase in electron acceptor strength upon substituting one RC≡C− by one N≡C− group can be quantified to an average of 380 mV. Replacing one RC≡C−C−C≡CR by a NC−C−CN fragment increases the average electron acceptor strength by 830 mV. A linear correlation (R^2 = 0.996) exists between the calculated adiabatic electron affinities (B3LYP, 6–31G**, Gaussian program[35]) and the first reduction potentials for TEE **1**, CEEs **3**–**8**, and TCNE (**2**).

The dimeric CEEs exhibit two reversible one-electron reduction steps, eventually followed by an irreversible third step. By comparing the values of the dimers with those of their analogous monomeric CEEs, it can be concluded that an increase in conjugation length results in an anodic shift and thus acceptor strength. This finding represents another example[2] for the efficiency of π-electron conjugation across buta-1,3-diynediyl fragments, a hot topic of current theoretical calculations.[39]

All donor-substituted CEEs give one or two reversible oxidation steps (except **17**, **22**, and **23**), depending on the number of DMA groups (Table 6). A reversible reduction (except for **19**) is followed by one or more, mainly irreversible reduction steps.

The CV data show that the DMA donor and CEE acceptor cores in monomeric donor-substituted CEEs are clearly conjugated. In a π-conjugated system, the presence of an electron-donating group hinders the electron reduction and an electron-withdrawing group makes the oxidation more difficult. The oxidation of the DMA unit in the TEEs is not influenced by the presence of other electron-accepting substituents (such as *p*-nitrophenyl) and has an average first oxidation potential of +0.44 V.[34b,40] In contrast, large shifts to more positive potentials are induced by the introduction of cyano groups in the CEEs. The highest first oxidation potential is obtained for **19** (+0.79 V). This is in agreement with the largest amount of CT from the donor to the acceptor moiety for this molecule within the CEE series, as observed by NMR spectroscopy and X-ray crystal structure analysis (vide supra).

The increase in the number of CN groups, with one DMA group present in the molecule, causes an approximately cumulative shift to more positive potentials for the oxidation of the DMA group. From (*E*)-**12** (1 CN), to **15** (2 CN), and to **19** (3 CN), the observed shifts of the oxidation potential are +120 mV, +230 mV, and +350 mV, respectively, relative to the TEE with one DMA group (oxidation potential +0.44 V[34b,40]). The difference in the first reduction potential between the donor-substituted CEEs and their parent CEEs also increases by the introduction of additional CN groups. The values shift by 60 mV, 90 mV, and 140 mV for (*E*)-**12**, **15**, and **19**, respectively, to more negative potentials relative to their DMA-free analogues **3** ($E_{red,1}$ = −1.58 V), **6**

Table 6. Cyclic voltammetry data of donor-substituted CEEs in CH_2Cl_2 (+0.1 M nBu_4NPF_6).[a] For an overview of the molecules, see structural formulae in the text.

	Cyclic voltammetry			Rotating disk voltammetry	
	E^o [V][b]	ΔE_p [mV][c]	E_p [V][d]	$E_{1/2}$ [V][e]	Slope [mV][f]
(*E*)-**12**	+0.56	80		+0.59 (1 e$^-$)	60
	−1.64	90		−1.70 (1 e$^-$)	70
			−2.26		
			−2.37		
(*Z*)-**12**	+0.56	75		+0.59 (1 e$^-$)	70
	−1.63	75		−1.67 (1 e$^-$)	75
			−2.25	−2.39 (2 e$^-$)	150
			−2.35		
13	+0.52	80		+0.55 (1 e$^-$)	70
	−1.64	100		−1.67 (1 e$^-$)	100
			−2.47		
15	+0.67	125		+0.67 (1 e$^-$)	70
	−1.24	125		−1.32 (1 e$^-$)	100
17			+0.63	+0.65 (2 e$^-$)	50
	−1.31	60		−1.35 (1 e$^-$)	70
			−2.02	−2.06	75
			−2.20		
18	+0.50	70		[g]	
	+0.58	70			
	−1.38	70			
			−1.95	−1.44 (1 e$^-$)	100
			−2.05		
			−2.20		
19	+0.79	65		+0.79 (1 e$^-$)	60
			−0.86	−0.85 (1 e$^-$)	60
20	+0.69	120		+0.70 (2 e$^-$)	[g]
	−0.74	60		−0.77 (1 e$^-$)	60
	−0.92	70		−0.95 (1 e$^-$)	60
			−2.25	−2.31 (2 e$^-$)	75
21	+0.72	70		+0.70[g]	
	−0.81	90		−0.88 (1 e$^-$)	80
			−1.75	−1.79 (2 e$^-$)	160
22			+0.56	+0.57 (2 e$^-$)	85
	−0.67	65		−0.67 (1 e$^-$)	70
			−1.39	−1.47 (1 e$^-$)	120
23			+0.50	+0.56 (2 e$^-$)	120
	−0.93	70		−0.94 (1 e$^-$)	70
	−1.49	60		−1.48 (1 e$^-$)	90
24	+0.61	65		+0.64 (2 e$^-$)	60
	+0.45	70		+0.46 (2 e$^-$)	60
	−0.89	75		−0.90 (2 e$^-$)	75
	−1.40	65		−1.40 (1 e$^-$)	60
	−1.50	70		−1.52 (1 e$^-$)	75

[a] Potentials versus the ferricinium/ferrocene couple. Working electrode: glassy carbon electrode; counter electrode: Pt; reference electrode: Ag/AgCl. [b] $E^o = (E_{pc} + E_{pa})/2$, where E_{pc} and E_{pa} correspond to the cathodic and anodic peak potentials, respectively. [c] $\Delta E_p = E_{ox} - E_{red}$, in which subscripts ox and red refer to the conjugated oxidation and reduction steps, respectively. [d] E_p = Irreversible peak potential at sweep rate v = 0.1 V s^{-1}. [e] $E_{1/2}$ = Half-wave potential. [f] Slope = Slope of the linearized plot of E versus $\log[I/(I_{lim}-I)]$. I_{lim} is the limiting current and I the current. [g] Electrode inhibition during oxidation. No plateau-limiting current could be observed.

($E_{red,1} = -1.15$ V), and **8** ($E_{red,1} = -0.72$ V). Both facts indicate an increase in interaction between the DMA donor and the CEE acceptor core with a larger number of CN groups. The differences in the reduction potential are relatively small compared to the average gain in acceptor strength of ~380 mV per additional cyano group (vide supra).

The shifts to more positive oxidation and more negative reduction potentials can be considered as a lowering and an elevation of the HOMO and LUMO levels, respectively. The constitutional isomers (*E*)-**12**, (*Z*)-**12**, and **13** have similar reduction potentials (~−1.64 V). The first oxidation potentials are identical for the *trans* D–A- ((*Z*)-**12**) and *cis* D–A-conjugated isomers ((*E*)-**12**), but less positive for geminally conjugated **13** (Table 6). The larger differences in the first oxidation potential indicate that the HOMO is more sensitive to a change in substitution pattern than the LUMO. This was confirmed by theoretical calculations.[41a]

Chromophore **22** shows hardly any interaction between the DMA and the tricyanovinyl acceptor groups. The first oxidation potential is only shifted by 60 mV to more positive potentials relative to the average potential for DMA oxidations in TEEs (+0.44 V[34b,40]). The first reduction potential of **22** is 190 mV more positive and the first oxidation potential 290 mV less positive than the corresponding potentials of **19**, which also contains a tricyanovinyl and DMA group. This clearly shows that there is much less D–A interaction in the expanded chromophore **22** than in highly conjugated, monomeric **19**.

Similarly, heterodimeric **23** shows rather isolated donor and acceptor parts. The oxidation potential is 130 mV less positive than the value for monomeric **17**, which contains a similar geminal donor and geminal acceptor substitution pattern. The first reduction potential is only 30 mV more negative than that of the related DMA-free heterodimer **10** ($E_{red,1} = -0.90$ V, Table 5). Both facts indicate that there is only weak interaction between the donor and acceptor parts separated by the extended spacer.

In heterotetrameric **24**, a distinction between two isolated DMA groups ($E_{ox} = +0.45$ V) and two DMA groups that interact with the CEE cores ($E_{ox} = +0.61$ V) is observed. This differentiation between the DMA groups is visible in the ^{1}H NMR spectrum (vide supra); it is also present in the related TEE dimer with four DMA groups ($E_{ox} = +0.37$ V and $E_{ox} = +0.54$ V).[42]

UV/Vis spectroscopy: A general feature of the UV/Vis spectra of the donor-substituted CEEs is their very intense and dominant CT band with transition dipole moments M up to 9.8 Debye (Figure 2; for the transition dipole moments, see Supporting Information). Thus, the spectrum of **19** features a CT band with a λ_{max} of 591 nm (2.10 eV) and a molar extinction coefficient of 43 800 M^{-1} cm^{-1} (Figure 2). Upon protonation of the DMA moiety with trifluoroacetic acid (TFA), the solution of **19** turns from blue to colorless and the longest wavelength absorption band disappears almost completely. The CT band can be fully regenerated upon neutralization with Et_3N. Comparison of **19** with its known alkyne-free analogue 4-(tricyanovinyl)-*N*,*N*-dimethylaniline ($\lambda_{max} = 530$ nm, $\varepsilon \approx 40\,000$ M^{-1} cm^{-1})[43] indicates a bathochromic shift of λ_{max} of 61 nm (0.24 eV) for **19**. Thus, the HOMO–LUMO gap is significantly reduced by the introduction of the ethynyl spacer.

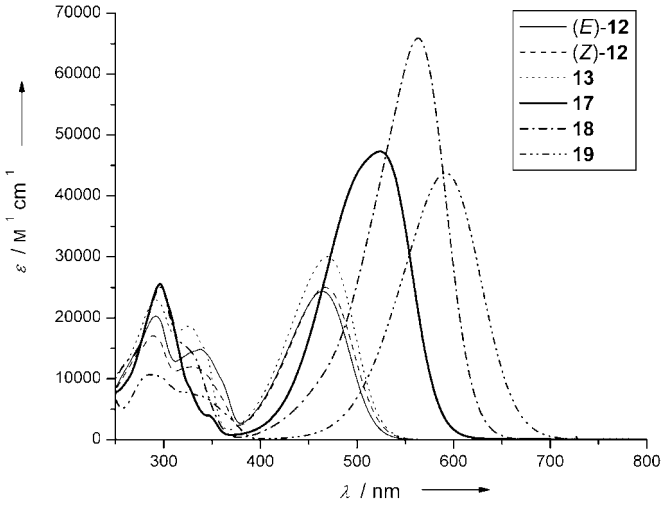

Figure 2. UV/Vis spectra of selected monomeric donor-substituted CEEs in $CHCl_3$.

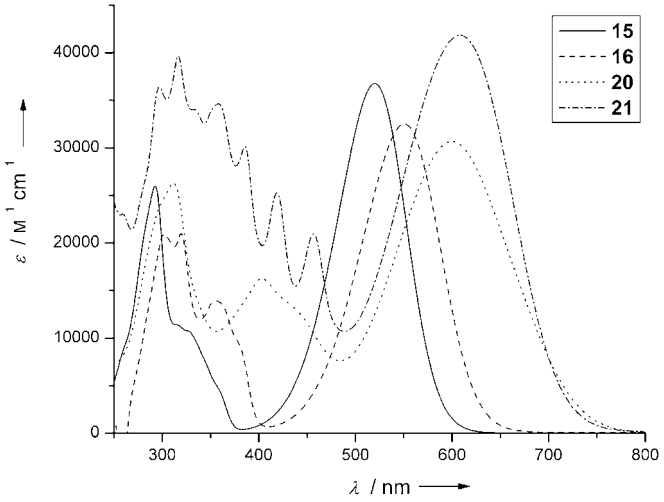

Figure 3. Shift of the CT band in the UV/Vis spectrum ($CHCl_3$) upon changing from monomeric donor-substituted CEEs **15** and **16** to the dimeric derivatives **20** and **21**.

The change from the monomeric donor-substituted CEEs to the more extended chromophores results in a red shift of the maximum (λ_{max}) of the CT absorption band. Changing from monomeric **15** to dimeric **20** (Figure 3) moves λ_{max} by 0.31 eV. Extending **15** by one ethynyl unit to give **16** results in a bathochromic shift of 0.13 eV. The dimerization of silyl-deprotected **16** to give **21** provides an additional shift of 0.21 eV. The structureless absorption spectrum of **20** changes by the insertion of an additional buta-1,3-diynediyl moiety (to **21**) into a spectrum with a remarkable fine structure of the higher energy absorption bands (Figure 3). The spectral data of all donor-substituted CEEs are summarized in Table 7.

Optical versus electrochemical HOMO–LUMO gap: A plot of the optical band gap, calculated from λ_{max} of the CT band

Table 7. Summary of the UV/Vis spectra of donor-substituted CEEs in $CHCl_3$ and electrochemical band gaps determined by CV in CH_2Cl_2.[a]

Compound	λ_{max} [nm (eV)]	λ_{end} [nm (eV)]	$\Delta(E_{ox,1}-E_{red,1})$ [V]
(*E*)-**12**	467 (2.65)	570 (2.18)	2.20
(*Z*)-**12**	464 (2.67)	570 (2.18)	2.19
13	470 (2.64)	575 (2.16)	2.16
15	520 (2.38)	660 (1.89)	1.91
16	551 (2.25)	730 (1.69)	-
17	524 (2.37)	700 (1.77)	1.94
18	563 (2.20)	685 (1.81)	1.88
19	591 (2.10)	750 (1.65)	1.65
20	600 (2.07)	860 (1.44)	1.43
21	608 (2.04)	870 (1.42)	1.53
22	734 (1.69)	1030 (1.20)	1.23
23	554 (2.24)	925 (1.34)	1.43
	649 (1.91)[b]		
24	548 (2.26)	925 (1.34)	1.34
	707 (1.75)[b]		

[a] The optical band gap is either determined from λ_{max} of the CT band or from the optical end-absorption λ_{end}. [b] Shoulder.

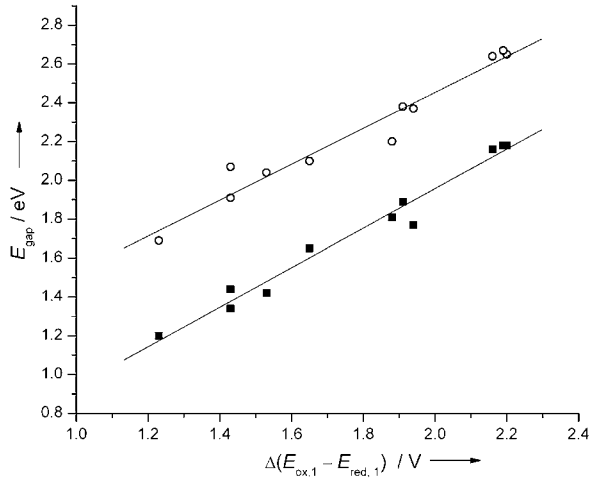

Figure 4. Linear correlation between the optical band gap E_{gap}, determined from λ_{max} (○) and λ_{end} (■), and $\Delta(E_{ox,1}-E_{red,1})$.

or the end-absorption λ_{end} in the UV/Vis spectrum, against the difference between the first oxidation potential and the first reduction potential in the CV (the electrochemical band gap, Table 7) shows a linear correlation ($R=0.976$ for λ_{end} and $R=0.987$ for λ_{max}) between the two quantities (Figure 4). This suggests that the same orbitals are involved in electrochemistry and in absorption spectroscopy. TD-B3LYP/6–31G** calculations had also indicated that the CT absorption bands in the UV/Vis spectra of donor-substituted CEEs are determined by HOMO–LUMO transitions.[41]

This correlation allows the use of the electrochemical data for the explanation of the features seen in the UV/Vis spectra. A decrease in the band gap of 0.28 eV for each additional CN group is observed (compare (*E*)-**12** to **15** and **19**). The CV data show that the oxidation potential becomes ~120 mV more positive and the reduction potential ~−380 mV less negative with each additional cyano group

(vide supra). The decrease of the HOMO–LUMO gap can therefore be mainly attributed to the lowering of the LUMO level rather than to the elevation of the HOMO level. However, the HOMO is more sensitive to the substitution pattern within the constitutional isomers.

In a π-conjugated system, the presence of an electron-donating group hinders the electron reduction and an electron-withdrawing group makes the oxidation more difficult (vide supra). This has severe implications on the size of the optical band gap: with more efficient π-conjugation in a molecule, the oxidation will get more difficult, that is, the HOMO level will be lowered. The more difficult reduction will result in a higher LUMO level. This means that within a series of constitutional isomers, the most conjugated molecule will have a larger band gap!

This principle can be demonstrated by comparing the constitutional isomers **17** and **18**. Chromophore **17** has four linearly conjugated D–A pathways, whereas **18** features two linearly and two cross-conjugated D–A pathways. Hence, D–A conjugation in **17** is more efficient. On the other hand, the longest wavelength absorption maximum λ_{max} of **18** is bathochromically shifted by 39 nm (0.17 eV) relative to **17** and has a much higher molar extinction coefficient (63800 vs 47300 $M^{-1}cm^{-1}$). The CV data indicate that the highest conjugated molecule **17** has a much lower HOMO level than **18**, which results in a larger band gap. B3LYP calculations show a more pronounced CT in the HOMO level of **17** than of **18**, which can explain the experimentally found energy lowering of this level.[41a]

Similarly, the lower band gap of geminally D–A-substituted **13** can be explained by the disfavored D–A cross-conjugation, resulting in an elevation of the HOMO level ($E_{ox,1}$ = +0.52 V for **13**, $E_{ox,1}$ = +0.56 V for **12**) and a lower band gap with respect to (*E*)- and (*Z*)-**12** with linear D–A conjugation pathways.

Now that it has been shown that an increase in D–A conjugation can lead to an increase of the band gap, the extremely small band gap of chromophore **22** (Figure 5) can be explained. Electrochemistry indicated a lack of interaction between the donor-substituted TEE part and the strongly accepting tricyanovinyl group in **22** (vide supra). With respect to **19**, which contains the same tricyanovinyl acceptor group and a DMA donor, but exhibits a larger amount of conjugation, the band gap is lowered with more than 0.40 eV! The end-absorption reaches into the near-IR (1030 nm, 1.20 eV).

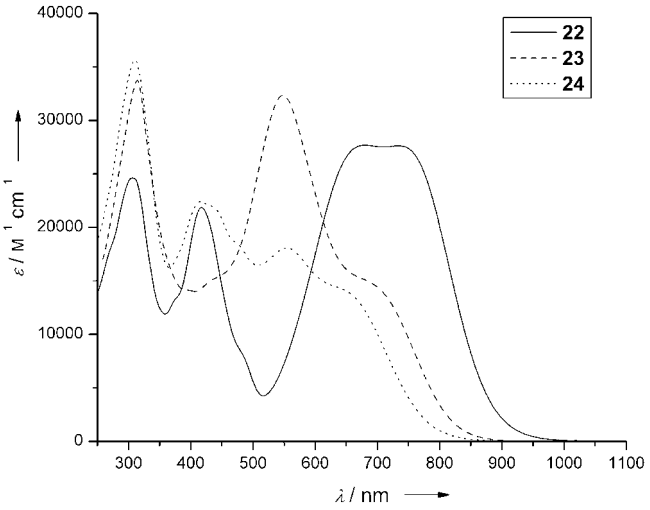

Figure 5. UV/Vis spectra of extended donor-substituted CEE chromophores in $CHCl_3$.

Additional proof for the rather isolated donor and acceptor parts in **22** and in **23** is obtained from the UV/Vis spectra. The spectrum of the bis-Si*i*Pr_3-protected analogue of bis-donor-substituted TEE **43** (Scheme 4) shows two peaks at 300 and 428 nm.[4] These bands can be recognized in the spectra of **22** and **23** (311, 416–434 nm). The low extinction coefficient of the CT band suggests little coupling between the donor and acceptor parts of the molecule.

The undisturbed strong electron acceptor and donor moieties cause a lowering of the LUMO level and an elevation of the HOMO level with respect to monomer **17**, resulting in a smaller band gap for **23**. Going from dimeric **23** to tetrameric **24**, the shoulder moves from 649 nm to 707 nm (shift of 0.16 eV), but the end-absorption remains approximately the same. The UV/Vis spectrum of tetrameric **24** is virtually identical to the spectrum of a dimeric TEE with four DMA groups[42] (which forms the core of **24**). The λ_{max} and end-absorption of **24** are 95 nm (0.48 eV) and 275 nm (0.57 eV) bathochromically shifted compared to this TEE dimer. Again, the relatively low extinction coefficient of the CT band suggests that the donor and acceptor parts are only weakly coupled.

The above examples show that the band gap can be tuned by insertion of acetylenic (and also olefinic) spacer units, which sometimes "insulate" strong donor and acceptor moieties. The presence of noninteracting donors and acceptors in one molecule can result in an extremely small HOMO–LUMO gap, but also give relatively small extinction coefficients. Contrary to chemical intuition, efficient conjugative interactions between donors and acceptors can increase the band gap.

Solvatochromism in the fluorescence and UV/Vis spectra: Some of the donor-substituted CEEs showed a bright yellow/orange fluorescence in hexane solutions. Molecule **18** displays the highest fluorescence intensity, with a quantum yield of 58% in hexane/$CHCl_3$ 19:1. All monodonor–monoacceptor-substituted CEEs are fluorescent. No quantum yields were determined for (*E*)-**12** and (*Z*)-**12** due to their photoisomerization in hexane. The geminally substituted derivative **13** also shows a good luminescence quantum yield of 39%.

The fluorescence is highly dependent on solvent polarity as shown in Table 8. The quantum yield is almost zero in the relatively polar solvent $CHCl_3$. An increase in the percentage of hexane in the solvent mixture results in a tremendous enhancement of the fluorescence efficiency. This solvatochromic behavior is observed for all fluorescent CEEs. Also,

Table 8. Fluorescence data for several donor-substituted CEEs. Quantum yields ϕ_F are measured against rhodamine 6G,[44] unless otherwise stated. λ_{ex} and λ_{em} are the excitation and emission wavelength, respectively.

	Solvent	λ_{ex} [nm]	$\lambda_{em,max}$ [nm]	ϕ_F	Stokes shift [cm^{-1}]
13[a]	hexane	340	481	0.39	487
15	hexane	480	528	0.044	1679
	hexane/$CHCl_3$ 9:1	480	581	0.006	3196
17	hexane/$CHCl_3$ 9:1	480	558	0.012	2529
	hexane/$CHCl_3$ 1:1	480	594	0.002	2850
18	hexane/$CHCl_3$ 19:1	[b]	570	0.58	1540
	hexane/$CHCl_3$ 9:1	[b]	582	0.45	1757
	hexane/$CHCl_3$ 1:1	[b]	620	0.054	2053
	$CHCl_3$		643	0.008	2210
19	hexane/$CHCl_3$ 19:1	540[c]	672	0.002	3672

[a] Reference: anthracene.[45] [b] Excitation at three different wavelengths 480, 485, 490 nm; quantum yield averaged. [c] Reference: sulforhodamine 101 ($\phi_F = 0.90$).[46]

an increase in the Stokes shift is measured upon changing to more polar solvents. Similarly, λ_{max} of the CT band in the UV/Vis spectra becomes red-shifted upon going from hexane to $CHCl_3$. Both effects can be explained by the excited state being more polar than the ground state.[47]

The absorption maxima of the DMA-substituted monocyanotriethynylethenes **12** and **13** have smaller solvent shifts upon changing from $CHCl_3$ to hexane (0.07–0.10 eV) than the CEEs with two or more cyano groups (0.17–0.20 eV). This suggests that a larger dipole moment change from the ground to the excited state occurs in the chromophores with more electron-accepting moieties (Table 9).

Table 9. Solvent effects in the UV/Vis spectra of several donor-substituted CEEs.

	λ_{max} [nm (eV)] in solvent				
	hexane	hexane/ $CHCl_3$ 19:1	hexane/ $CHCl_3$ 9:1	hexane/ $CHCl_3$ 1:1	$CHCl_3$
(*E*)-**12**	453 (2.74)				467 (2.65)
(*Z*)-**12**	448 (2.77)				464 (2.67)
13	458 (2.71)				470 (2.64)
15	485 (2.56)		490 (2.53)		520 (2.38)
17			489 (2.54)	508 (2.44)	524 (2.37)
18		524 (2.37)	528 (2.35)	550 (2.25)	563 (2.20)
19		539 (2.30)	543 (2.28)	572 (2.16)	591 (2.10)

The centrosymmetric chromophore **18** has no dipole moment, but shows solvatochromic effects similar to those of the noncentrosymmetric donor-substituted CEEs. According to the Franck–Condon principle,[48] the excited state of **18** should have the same geometry as the ground state and therefore no dipole moment. A change in the dipole moment upon electronic excitation can therefore not be used to explain the observed solvatochromism. However, a similar solvatochromism has been observed in other centrosymmetric molecules. These effects have mainly been attributed to a localized excitation in one part of a molecule, generating a dipole moment in the excited state, while conserving the geometry[49] or to a solvent-induced symmetry breaking.[50]

The UV/Vis spectrum of **18** (Figure 2, Table 7) indicates a strong CT from the ground to the excited state. The charge from the donors is transported to the cyano acceptors, generating a partially positive charge on the donors and a negative charge on the acceptors, that is, a quadrupole. Therefore, we propose that the increase in electric moment from the ground to the excited state through a change in the quadrupole moment is the most likely explanation for the solvatochromic effects observed for **18**.[51] Localized excitation in one part of the molecule or solvent-induced symmetry breaking are unlikely in a small, conjugated molecule such as **18**.

Two-photon absorption: The donor-substituted CEEs show good π-conjugation, large transition dipole moments (up to 9.8 Debye, see Supporting Information), large changes in electric moment from the ground to the excited state, and small band gaps. These are all prerequisites for good NLO properties.[6b,14] Therefore, two-photon absorption (TPA) measurements were carried out on compound **17**, using the *Z* scan technique.[52] Due to the limited wavelength range of the laser, CEEs **19** and **18** could not be measured. Since compound **20** shows a weak (one-photon) absorption around 800–900 nm, the TPA cross-section cannot be determined at 900 nm. For CEE **17**, a cross-section value of $\sigma_2 = 8.8 \times 10^{-49}$ $cm^4 s$ per photon in 1,1,2,2-tetrachloroethane at 900 nm was measured. This value is approximately three times higher than the value for the AF-50 standard (3.0×10^{-49} $cm^4 s$ per photon at 796 nm in benzene).[53a] These TPA cross-sections are difficult to compare, since the values are highly dependent on the experimental setup, the monitoring wavelength, the solvent used, the intensity level, and especially on the pulse duration. Nevertheless, this first TPA cross-section value indicates the high potential of the donor-substituted CEEs for nonlinear optical applications, considering the small size and small number of functional groups.

Conclusion

Following initial reports on some isolated cyanoethynylethenes (CEEs)[8–11] a comprehensive family of these chromophores has been prepared. With increasing number of CN groups, the electron-accepting properties as determined by electrochemistry, become strongly enhanced. In fact, the dimeric CEEs start to rival the benchmark tetracyanoethene (TCNE) in their acceptor capacity. Based on the data in this paper, we actually predict that the still elusive, dimeric CEE with six peripheral CN groups will be similar or possibly even superior to TCNE in its electron-accepting capacity. As a distinct advantage over TCNE, the CEEs are versatile building blocks for integration into larger entities and their scaffolding power has been proven by the synthesis of extended, DMA (*N*,*N*-dimethylanilino) donor-functionalized charge-transfer chromophores. The charge-transfer conjugation pathways in these molecules were comprehensively investigated by means of X-ray crystallography, NMR spectro-

scopy, electrochemistry, and theoretical calculations. In CEEs, *cis* donor–acceptor conjugation is more effective than *trans* conjugation and both are far superior to geminal cross-conjugation. The conjugation effectiveness was particularly nicely revealed by large changes in the first oxidation and reduction potentials of the donor-substituted CEEs with respect to the isolated donor and acceptor moieties. According to the electrochemical data, differences between the band gaps of constitutional isomers observed by UV/Vis spectroscopy can mainly be explained by a change in the energetic level of the HOMO of the molecules. The higher conjugated molecules show a lower HOMO level, which leads to a larger band gap! By the introduction of acetylenic spacers between the donor and the acceptor parts in chromophores **22**–**24**, the conjugation in the molecules was diminished, which resulted in very small band gaps. This shows that the generally accepted rule that more π-conjugation leads to a bathochromic shift in the UV/Vis spectrum is not always valid.[41a,54] On the other hand, the reduced amount of coupling between the donor and acceptor parts also results in a lower transition dipole moment and molar absorption coefficient. Thus, this investigation has provided new insights into conjugation effects in strong charge-transfer chromophores and useful guidelines for tuning the band gaps of such systems. Finally, the facts that the donor-substituted CEEs can be sublimed without decomposition and **17** shows a high value for the two-photon absorption cross-section make these compounds very promising for applications in optoelectronic devices.

Experimental Section

Materials and general methods: Chemicals were purchased from Acros, Aldrich, Fluka, and GFS and used as received. THF was distilled from Na/benzophenone. CH_2Cl_2 was distilled from CaH_2. All reactions except the oxidative couplings were carried under an inert atmosphere by applying a positive pressure of Ar. Compounds **5**,[9a] **25**,[15] **26**,[16] **27**,[17] (3-bromopropynyl)triisopropylsilane,[18] **30**,[21] **31**,[15] **32** and **33**,,[17] **34**, **36**, and **37**,[29] *N*,*N*-dimethyl-4-ethynylaniline and **39**,[28] diethyl 1-chloro-1-cyanomethylphosphonate,[30] **42** and **43**[31] were prepared according to literature procedures. Protocols for the following compounds are included in the Supporting Information: 4-(triisopropylsilyl)but-3-ynenitrile, **35**, **38**, **40**, (*E*)- and (*Z*)-**41**, and **45**. The Hay catalyst was prepared from CuCl (0.065 g, 0.65 mmol) and TMEDA (0.080 g, 0.70 mmol) in CH_2Cl_2 (5.0 mL), resulting in a concentration of 0.13 mmol mL^{-1}. Column chromatography (CC) and plug filtrations were carried out with Fluka SiO_2 60 (particle size 40–63 μm, 230–400 mesh) and distilled technical solvents. Reversed-phase column chromatography was carried out with SiO_2 100 C18-Reversed-Phase (particle size 40–63 μm) from Fluka with an overpressure of about 0.3 bar and distilled technical solvents. Size exclusion chromatography (GPC) was carried out with Bio-beads S-X3 and S-X1 from the company Bio-Rad and distilled technical solvents. Melting points (m.p.) were measured in open capillaries with a Büchi Melting Point B540 apparatus and are uncorrected. ^{1}H NMR and ^{13}C NMR spectra were measured on Varian Gemini 200 or 300 MHz spectrometers. Chemical shifts are reported in ppm downfield from $SiMe_4$, using the solvent's residual signal as an internal reference. Coupling constants (J) are given in Hz. The resonance multiplicity is described as s (singlet), d (doublet), t (triplet), and m (multiplet). Infrared spectra (IR) were recorded on a Perkin–Elmer FT1600 spectrometer or a Perkin–Elmer Spectrum BX II. UV/Vis spectra were recorded on a Varian CARY-5 or Varian CARY-500 spectrophotometer. The spectra were measured in $CHCl_3$ in a quartz cuvette of 1 cm. The absorption wavelengths are reported in nm with the extinction coefficient in M^{-1} cm^{-1} in brackets. Shoulders are indicated as sh. Fluorescence spectra were measured on a Jobin Yvon Horiba Spex Fluorolog 3 spectrophotometer. Quantum yields were determined vs. rhodamine 6G ($\phi_F = 0.95$),[44] sulforhodamine 101 ($\phi_F = 0.90$),[46] or anthracene ($\phi_F = 0.32$).[45] EI mass spectra were measured at 70 eV on a Hitachi–Perkin–Elmer VG-TRIBRID spectrometer. High-resolution (HR) FT-MALDI spectra were measured on an Ionspec Fourier Transform instrument with 2,5-dihydroxybenzoic acid (DHB) or *trans*-2-[3-(4-*tert*-butylphenyl)-2-methylprop-2-enylidene]malononitrile (DCTB) in MeOH/H_2O as matrix, and the compound in CH_2Cl_2 (two layer technique). The most important signals are reported in m/z units, with M as the molecular ion and the intensities in brackets. Elemental analyses were performed by the Mikrolabor at the Laboratorium für Organische Chemie, ETH Zürich.

Electrochemistry: Electrochemistry measurements were carried out at 20 °C in CH_2Cl_2 containing 0.1 M nBu$_4$NPF$_6$ in a classical three-electrode cell. CH_2Cl_2 was purchased in spectroscopic grade from Merck, dried over molecular sieves (4 Å), and stored under Ar prior to use. nBu$_4$NPF$_6$ was purchased in electrochemical grade from Fluka and used as received. The working electrode was a glassy carbon disk electrode (3 mm in diameter) used either motionless for CV (0.1 to 10 V s^{-1}) or as rotating disk electrode for rotating disk voltammetry (RDV). The auxiliary electrode was a platinum wire, and the reference electrode was an aqueous Ag/AgCl electrode. All potentials are referenced to the ferricinium/ferrocene (Fc^+/Fc) couple, used as an internal standard. The accessible range of potentials on the glassy carbon electrode was +1.4 to −2.4 V versus Fc^+/Fc in CH_2Cl_2. The electrochemical cell was connected to a computerized multipurpose electrochemical device AUTOLAB (Eco Chemie BV, Utrecht, The Netherlands), and controlled by the GPSE software, running on a personal computer.

Two-photon absorption (TPA): TPA cross-sections were measured by using an open-aperture Z scan method.[52] A mode-locked Ti:Sapphire laser (Spectra-Physics, Mai Tai, ~100 fs, 80 MHz) was used as the laser source. The repletion rate of the pulses was reduced to 100 Hz by using a mechanical chopper for all measurements. After passing through an f= 12 cm lens, the laser beam was focused and passed through a 5 mm quartz cell filled with the sample solution (10^{-3}–10^{-2} M). The laser intensity at the sample was in the range of 0.5–5 GW cm^{-2}. The transmitted laser beam from the sample cell was detected by using a photodiode, while changing position of the sample cell along the beam direction (Z axis). The two-photon cross-section was estimated by simulation.[52] AF-50 and ZnSe were used as references.[53]

X-ray analysis: The crystal structures of (*Z*,*Z*)-**11**, **18**, and **19** are described in references [12] and [13]. CCDC-182715, 207516, and 207517 contain the supplementary crystallographic data for this paper. These data can be obtained free of charge from The Cambridge Crystallographic Data Centre via www.ccdc.cam.ac.uk/data_request/cif.

2,3-Bis[(triisopropylsilyl)ethynyl]-5-(triisopropylsilyl)pent-2-en-4-ynenitrile (3): iPr$_2$EtN (12 μL, 0.070 mmol) was added to a solution of **27** (17.4 mg, 0.0445 mmol) and 4-(triisopropylsilyl)but-3-ynenitrile (14.9 mg, 0.0673 mmol) in EtOH (1.5 mL). After heating for 8 h at 80 °C, the solution was passed through a plug (CH_2Cl_2/hexane 1:1), affording **3** (26.0 mg, 97 %) as a colorless oil. ^{1}H NMR (300 MHz, $CDCl_3$): δ = 1.10 ppm (m, 63 H); ^{13}C NMR (75 MHz, $CDCl_3$): δ = 11.19, 11.22, 11.25, 18.60, 18.66, 18.69, 98.99, 101.72, 101.73, 106.30, 106.74, 107.60, 108.62, 115.10, 124.70 ppm; IR (CCl_4): $\tilde{\nu}$ = 2945, 2892, 2867, 2226, 1463, 1384, 1368, 1289, 1236, 1186, 1071, 1015, 997, 919, 883 cm^{-1}; UV/Vis ($CHCl_3$): λ (ε) = 300 (12000), 341 (25400), 355 nm (26300); EI-MS (70 eV): m/z (%): 550 (100) [M−iPr]$^+$, 508 (49) [M+H−2iPr]$^+$; elemental analysis calcd (%) for $C_{36}H_{63}NSi_3$ (594.16): C 72.77, H 10.69, N 2.36; found: C 72.75, H 10.57, N 2.15.

(*E*)- and (*Z*)-2,3-Bis[(triisopropylsilyl)ethynyl]-5-(triethylsilyl)pent-2-en-4-ynenitrile (4): iPr$_2$EtN (59 μL, 0.35 mmol) was added to a solution of **26** (99.7 mg, 0.286 mmol) and 4-(triisopropylsilyl)but-3-ynenitrile (76.0 mg, 0.345 mmol) in EtOH (6 mL). After stirring for 5 min at RT, the mixture was directly subjected to CC (hexane/CH_2Cl_2 2:1), which af-

forded (*E*)-**28** (18 mg, 15%) and a mixture of **4** and (*Z*)-**28**. The latter mixture was subjected to reversed-phase CC (MeCN/CH_2Cl_2 5:1), affording **4** (74 mg, 47%) and (*Z*)-**28** (33 mg, 27%). ^{1}H NMR (300 MHz, $CDCl_3$): $\delta = 0.68$ (m, 6H), 1.02 (m, 9H), 1.10 ppm (m, 42H); ^{13}C NMR (75 MHz, $CDCl_3$): $\delta = 4.13$, 7.44, 7.48, 11.22, 11.25, 18.59, 18.65, 18.68, 98.95, 98.99, 100.88, 100.98, 101.56, 101.64, 106.45, 106.65, 107.02, 107.39, 107.56, 107.68, 108.78, 108.91, 114.98, 115.05, 124.61, 124.93 ppm; IR (CCl_4): $\tilde{\nu} = 2960$, 2945, 2891, 2867, 2226, 1463, 1415, 1384, 1368, 1291, 1235, 1187, 1071, 1014, 997, 920, 883 cm^{-1}; UV/Vis ($CHCl_3$): λ (ε) = 279 (sh, 7400), 296 (10700), 340 (25500), 354 nm (26300); EI-MS (70 eV): *m*/*z* (%): 551 (5) $[M]^+$, 508 (100) $[M-i\mathrm{Pr}]^+$, 466 (47) $[M+\mathrm{H}-2i\mathrm{Pr}]^+$; HR-EI-MS: *m*/*z* calcd for $C_{30}H_{50}NSi_3^+$: 508.3251; found: 508.3240 $[M-i\mathrm{Pr}]^+$.

(*Z*)- and (*E*)-3-ethynyl-5-(triisopropylsilyl)-2-[(triisopropylsilyl)ethynyl]-pent-2-en-4-ynenitrile ((*Z*)-28 and (*E*)-28): $i\mathrm{Pr}_2\mathrm{EtN}$ (59 μL, 0.35 mmol) was added to a solution of **26** (100 mg, 0.287 mmol) and 4-(triisopropylsilyl)but-3-ynenitrile (76.4 mg, 0.345 mmol) in EtOH (6 mL). After stirring for 5 min at RT, the mixture was directly subjected to CC (hexane/CH_2Cl_2 2:1). The solvent was evaporated in vacuo. The residue was dissolved in MeOH/THF (1:1, 20 mL), and K_2CO_3 (18 mg, 0.13 mmol) was added. After 10 min, reversed phase TLC (MeOH) showed complete deprotection and H_2O and Et_2O were added. The aqueous layer was extracted with Et_2O. The collected organic fractions were washed with sat. NaCl solution and dried with $MgSO_4$. CC (hexane/CH_2Cl_2 2:1) afforded (*Z*)-**28** (58 mg, 46%) as a colorless, unstable solid and (*E*)-**28** (35 mg, 29%) as an unstable oil.

*Data for (Z)-**28***: ^{1}H NMR (300 MHz, $CDCl_3$): $\delta = 1.12$ (m, 42H), 3.708 ppm (s, 1H); ^{13}C NMR (75 MHz, $CDCl_3$): $\delta = 1.17$, 11.21, 18.62, 78.96, 89.99, 98.56, 100.65, 108.39, 108.40, 109.15, 114.45, 124.40 ppm; IR (CCl_4): $\tilde{\nu} = 3306$, 2945, 2919, 2893, 2867, 2224, 2103, 1463, 1384, 1368, 1288, 1234, 1188, 1071, 1019, 997, 984, 920, 883 cm^{-1}; UV/Vis ($CHCl_3$): λ (ε) = 263 (5000), 334 (21400), 348 nm (22000); EI-MS (70 eV): *m*/*z* (%): 394 (100) $[M-i\mathrm{Pr}]^+$, 352 (29) $[M+\mathrm{H}-2i\mathrm{Pr}]^+$; HR-EI-MS: *m*/*z* calcd for $C_{24}H_{36}NSi_2^+$: 394.2386; found: 394.2375 $[M-i\mathrm{Pr}]^+$.

*Data for (E)-**28***: ^{1}H NMR (300 MHz, $CDCl_3$): $\delta = 1.11$ (m, 42H), 3.715 ppm (s, 1H); ^{13}C NMR (75 MHz, $CDCl_3$): $\delta = 11.24$, 18.66, 79.02, 88.85, 98.64, 100.98, 108.10, 108.74, 109.82, 114.94, 123.39 ppm; IR (CCl_4): $\tilde{\nu} = 3307$, 2945, 2892, 2867, 2224, 2101, 1463, 1384, 1367, 1287, 1173, 1071, 1018, 998, 920, 883 cm^{-1}; UV/Vis ($CHCl_3$): λ (ε) = 286 (8500), 331 (20200), 345 nm (21500); EI-MS (70 eV): *m*/*z* (%): 394 (72) $[M-i\mathrm{Pr}]^+$, 352 (93) $[M+\mathrm{H}-2i\mathrm{Pr}]^+$; HR-EI-MS: *m*/*z* calcd for $C_{24}H_{36}NSi_2^+$: 394.2386; found: 394.2373 $[M-i\mathrm{Pr}]^+$.

2-{1-[(Triisopropylsilyl)ethynyl]-3-(trimethylsilyl)prop-2-ynylidene}malononitrile (6): A mixture of **25** (750 mg, 2.45 mmol), $CH_2(CN)_2$ (243 mg, 3.67 mmol), and Al_2O_3 (activity II-III, 1.10 g) in CH_2Cl_2 (2 mL) was heated to reflux for 50 min. The mixture was extracted with CH_2Cl_2 and subsequently passed through a plug (CH_2Cl_2). The filtrate was evaporated in vacuo, affording **6** (738 mg, 85%) as a dark yellow oil. ^{1}H NMR (300 MHz, $CDCl_3$): $\delta = 0.30$ (s, 9H), 1.13 ppm (m, 21H); ^{13}C NMR (75 MHz, $CDCl_3$): $\delta = 1.11$, 10.90, 18.31, 96.77; 97.85, 99.65, 111.73, 111.77, 116.07, 117.54, 134.12 ppm; IR ($CHCl_3$): $\tilde{\nu} = 2947$, 2868, 2231, 2139, 1501, 1463, 1296, 1253, 1177, 1005, 882, 851 cm^{-1}; UV/Vis ($CHCl_3$): λ (ε) = 305 (16700), 324 nm (15900); EI-MS (70 eV): *m*/*z* (%): 310 (100) $[M-\mathrm{H}-i\mathrm{Pr}]^+$; HR-FT-MALDI-MS (DHB): *m*/*z* calcd for $C_{20}H_{31}N_2Si_2^+$: 355.2026; found: 355.2021 $[M+\mathrm{H}]^+$.

(*E*)-2,3-Bis[(triisopropylsilyl)ethynyl]but-2-enedinitrile (7): $[PdCl_2(PPh_3)_2]$ (7.2 mg, 0.010 mmol) and CuI (3.0 mg, 0.016 mmol) were added to a degassed solution of **30** (50 mg, 0.21 mmol), $i\mathrm{Pr}_2\mathrm{NH}$ (129 mg, 0.18 mL, 1.3 mmol) and $i\mathrm{Pr}_3\mathrm{SiC}{\equiv}\mathrm{CH}$ (116 mg, 0.14 mL, 0.63 mmol) in THF (4 mL). The mixture was stirred for 48 h at RT under Ar and subsequently passed through a plug (CH_2Cl_2/hexane 1:1). The solvent was evaporated and the oily mixture dried for 18 h at 10^{-2} Torr. CC (CH_2Cl_2/hexane 1:1) resulted in **7** (29 mg, 30%) as a light yellow solid. M.p. > 250°C (decomp); ^{1}H NMR (300 MHz, $CDCl_3$): $\delta = 1.12$ ppm (m, 42H); ^{13}C NMR (75 MHz, $CDCl_3$): $\delta = 10.89$, 18.34, 97.27, 112.87, 114.42, 114.97 ppm; IR (CCl_4): $\tilde{\nu} = 2946$, 2892, 2867, 2227, 2154, 2062, 1462, 1385, 1368, 1235, 1189, 1071, 1019, 997, 978, 919, 883 cm^{-1}; UV/Vis ($CHCl_3$): 340 (sh, 14600), 351 nm (16000); EI-MS (70 eV): *m*/*z* (%): 439 (7) $[M+\mathrm{H}]^+$, 395 (100) $[M-i\mathrm{Pr}]^+$; elemental analysis calcd (%) for $C_{26}H_{42}N_2Si_2$ (438.80): C 71.71, H 9.65, N 6.38; found: C 71.09, H 9.55, N 6.23.

2-Cyano-3-[(triisopropylsilyl)ethynyl]but-2-enedinitrile (8): *n*BuLi (1.27 mL, 1.6 M in hexane, 2.03 mmol) was added to a cold solution (0°C) of $i\mathrm{Pr}_3\mathrm{SiC}{\equiv}\mathrm{CH}$ (0.45 mL, 2.0 mmol) in THF (3.0 mL). After stirring for 15 min, the solution was added to a cold solution (0°C) of CuBr (291 mg, 2.03 mmol) in THF (10 mL). After stirring for 1 h at 0°C, a solution of TCNE (200 mg, 1.56 mmol) in THF (2.5 mL) was added. The mixture was stirred for 1 h at RT, after which it was heated to 50°C for 45 min. The solvent was evaporated and the remaining extracted with hexane. The solvent was evaporated and the yellow oily solid extracted in the cold with MeCN. The resulting dark oil was rapidly filtered through a short plug (CH_2Cl_2), yielding **8** (146 mg, 33%) as a yellow oil. ^{1}H NMR (300 MHz, $CDCl_3$): $\delta = 1.15$ ppm (m, 21H); ^{13}C NMR (75 MHz, $CDCl_3$): $\delta = 11.10$, 18.50, 96.77, 103.19, 109.59, 109.74, 110.66, 122.21, 126.00 ppm; IR (CCl_4): $\tilde{\nu} = 2948$, 2893, 2868, 2222, 2150, 1525, 1462, 1386, 1370, 1285, 1167, 997, 972, 920, 883 cm^{-1}; UV/Vis ($CHCl_3$): λ (ε) = 297 (9300), 330 nm (11500); EI-MS (70 eV): *m*/*z* (%): 283 (9) $[M]^+$, 240 (24) $[M-i\mathrm{Pr}]^+$, 212 (44) $[M-i\mathrm{PrSi}]^+$; HR-EI-MS: *m*/*z* calcd for $C_{16}H_{21}N_3Si^+$: 283.1505; found: 283.1504 $[M]^+$.

3,8-Bis[(triisopropylsilyl)ethynyl]-2,9-dicyanodeca-2,8-diene-4,6-diynedinitrile (9): MeOH/THF 5:1 (300 mL) was added to **6** (500 mg, 1.41 mmol). After stirring for 10 min at RT, CH_2Cl_2 (200 mL) and H_2O (200 mL) were added. The aqueous layer was extracted with CH_2Cl_2, and the collected organic layers were washed twice with sat. NaCl solution. After drying with $MgSO_4$ and concentration to ~200 mL, $Cu(OAc)_2$ (520 mg, 2.86 mmol) was added. After stirring for 18 h at RT, the mixture was passed through a plug (CH_2Cl_2). Afterwards, GPC (CH_2Cl_2) and subsequent fast CC (CH_2Cl_2) resulted in **9** (88 mg, 22%) as a yellow solid. M.p. 75–77°C; ^{1}H NMR (300 MHz, $CDCl_3$): $\delta = 1.13$ ppm (m, 42H); ^{13}C NMR (75 MHz, $CDCl_3$): $\delta = 10.90$, 18.34, 81.56, 86.27, 98.24, 99.83, 111.14, 111.17, 120.13, 131.28 ppm; IR (KBr): $\tilde{\nu} = 2944$, 2892, 2864, 2228, 2140, 1499, 1462, 1385, 1368, 1286, 1173, 1159, 1069, 1019, 997, 985, 920, 881, 709, 676 cm^{-1}; UV/Vis ($CHCl_3$): λ (ε) = 316 (27500), 330 (27000), 356 (sh, 23300), 391 nm (17300); FT-MALDI-MS (DCTB): *m*/*z*: 608 $[M+2\mathrm{Na}]^+$, 585 $[M+\mathrm{Na}]^+$; HR-FT-MALDI-MS: *m*/*z* calcd for $C_{34}H_{42}N_4Si_2Na^+$: 585.2846; found: 585.2847 $[M+\mathrm{Na}]^+$.

2-{9-(Triisopropylsilyl)-1,6,7-tris[(triisopropylsilyl)ethynyl]non-6-ene-2,4,8-triynylidene}malononitrile (10): MeOH/THF 5:1 (18 mL) was added to **6** (30 mg, 0.085 mmol). After stirring for 10 min at RT, CH_2Cl_2 (20 mL) and H_2O (20 mL) were added. The aqueous layer was extracted with CH_2Cl_2, and the collected organic layers were washed twice with sat. NaCl solution. After drying with $MgSO_4$ and concentration to ~30 mL, **31** (123 mg, 0.208 mmol) and $Cu(OAc)_2$ (106 mg, 0.584 mmol) were added. After stirring for 42 h at RT, the mixture was passed through a short plug (CH_2Cl_2). CC (CH_2Cl_2/hexane 1:3) and subsequent GPC (CH_2Cl_2) resulted in **10** (22 mg, 27%) as a yellow oil. ^{1}H NMR (300 MHz, $CDCl_3$): $\delta = 1.10$ ppm (m, 84H); ^{13}C NMR (75 MHz, $CDCl_3$): $\delta = 11.04$, 11.10, 11.19, 18.45, 18.51, 18.58, 18.61, 78.12, 79.77, 89.99, 91.19, 97.18, 98.99, 100.49, 103.27, 103.32, 105.39, 107.90, 111.51, 111.80, 114.44, 116.49, 123.37, 129.74, 132.66 ppm; IR ($CHCl_3$): $\tilde{\nu} = 2960$, 2892, 2867, 2152, 2133, 1724, 1602, 1500, 1463, 1379, 1367, 1261, 1180, 1094, 1073, 1010, 882 cm^{-1}; UV/Vis ($CHCl_3$): 331 (28400), 340 (28100), 355 (27000), 377 (sh, 15700), 443 (sh, 9200), 477 nm (10400); FT-MALDI-MS (DHB): *m*/*z*: 896 $[M+\mathrm{Na}]^+$, 874 $[M+\mathrm{H}]^+$, 830 $[M-i\mathrm{Pr}]^+$; HR-FT-MALDI-MS: *m*/*z* calcd for $C_{54}H_{84}N_2Si_4Na^+$: 895.5609; found: 895.5603 $[M+\mathrm{Na}]^+$.

(2*Z*,8*Z*)-2,3,8,9-Tetrakis[(triisopropylsilyl)ethynyl]deca-2,8-diene-4,6-diynedinitrile ((*Z*,*Z*)-11): Hay catalyst (0.44 mL, 0.057 mmol) was added to a solution of (*Z*)-**28** (25.5 mg, 0.0582 mmol) in CH_2Cl_2 (15 mL). After stirring for 3 h at RT, the solvent was evaporated in vacuo. CC (hexane/CH_2Cl_2 2:1) afforded (*Z*,*Z*)-**11** (23.2 mg, 91%) as a bright yellow soild. M.p. > 130°C (decomp); ^{1}H NMR (300 MHz, $CDCl_3$): $\delta = 1.12$ ppm (m, 84H); ^{13}C NMR (75 MHz, $CDCl_3$): $\delta = 11.18$, 11.20, 18.61, 82.28, 84.50, 98.76, 99.22, 109.41, 110.72, 110.84, 114.27, 123.33 ppm; IR (CCl_4): $\tilde{\nu} =$ 2946, 2892, 2867, 2224, 2133, 1462, 1385, 1368, 1285, 1231, 1189, 1099, 1071, 1019, 997, 920, 883 cm^{-1}; UV/Vis ($CHCl_3$): 298 (sh, 17700), 317 (20500), 335 (22000), 353 (21800), 372 (18700), 391 (18600), 424 nm (20400); FT-MALDI-MS (DHB): *m*/*z*: 896 $[M+\mathrm{Na}]^+$, 874 $[M+\mathrm{H}]^+$, 830

$[M-i\mathrm{Pr}]^+$; HR-FT-MALDI-MS: *m/z* calcd $C_{54}H_{84}N_2Si_4Na^+$: 895.5609; found: 895.5608 $[M+\mathrm{Na}]^+$.

(2*E*,8*E*)-2,3,8,9-Tetrakis[(triisopropylsilyl)ethynyl]deca-2,8-diene-4,6-diynedinitrile ((*E*,*E*)-11): Hay catalyst (0.27 mL, 0.035 mmol) was added to a solution of (*E*)-**28** (15.4 mg, 0.0352 mmol) in CH_2Cl_2 (10 mL). After stirring for 3 h at RT, the solvent was evaporated in vacuo. CC (hexane/CH_2Cl_2 2:1), afforded (*E*,*E*)-**11** (13 mg, 85%) as a yellow oil. ^{1}H NMR (300 MHz, $CDCl_3$): $\delta=1.11$ ppm (m, 84H); ^{13}C NMR (75 MHz, $CDCl_3$): $\delta=11.26$, 18.69, 82.28, 83.43, 99.22, 99.86, 109.12, 111.03, 111.63, 114.64, 122.28 ppm; IR (CCl_4): $\tilde{\nu}=2946$, 2892, 2867, 2219, 2186, 2140, 1463, 1384, 1368, 1283, 1261, 1234, 1178, 1073, 1019, 998, 920, 883 cm^{-1}; UV/Vis ($CHCl_3$): λ (ε)=286 (sh, 11900), 317 (sh, 16900), 351 (21700), 371 (23300), 389 (22000), 421 nm (25000); FT-MALDI-MS (DHB): *m/z*: 896 $[M+\mathrm{Na}]^+$, 874 $[M+\mathrm{H}]^+$, 830 $[M-i\mathrm{Pr}]^+$; HR-FT-MALDI-MS: *m/z* calcd for $C_{54}H_{84}N_2Si_4Na^+$: 895.5609; found: 895.5600 $[M+\mathrm{Na}]^+$.

(*E*)-2,3-Bis{[4-(dimethylamino)phenyl]ethynyl}but-2-enedinitrile (18): $[PdCl_2(PPh_3)_2]$ (7.2 mg, 0.010 mg) and CuI (3.0 mg, 0.016 mmol) were added to a degassed solution of **30** (50 mg, 0.21 mmol), *N*,*N*-dimethyl-4-ethynylaniline (184 mg, 1.27 mmol), and $i\mathrm{Pr}_2\mathrm{NH}$ (129 mg, 0.18 mL, 1.3 mmol) in THF (5 mL). The mixture was stirred for 4 d at RT under Ar and subsequently passed through a plug (CH_2Cl_2). Recrystallization from CH_2Cl_2/hexane resulted in **18** (40 mg, 52%) as a blue/green metallic solid. M.p. 258°C; ^{1}H NMR (300 MHz, $CDCl_3$): $\delta=3.06$ (s, 12H), 6.65 (d, $J=9.0$ Hz, 4H), 7.46 ppm (d, $J=9.0$ Hz, 4H); ^{13}C NMR (75 MHz, $CDCl_3$): $\delta=40.11$, 84.37, 106.47, 108.97, 109.96, 111.58, 114.08, 133.93, 151.42 ppm; IR (KBr): $\tilde{\nu}=3445$, 2923, 2852, 2156, 1599, 1527, 1443, 1374, 1345, 1227, 1191, 1101, 1060, 940, 810 cm^{-1}; UV/Vis ($CHCl_3$): λ (ε)=266 (sh, 13400), 297 (25000), 325 (sh, 15000), 563 (65900); ($CHCl_3$/hexane 1:1): 263 (sh, 13700), 293 (25800), 319 (sh, 15400), 550 nm (68500); UV/Vis ($CHCl_3$/hexane 1:9): $\tilde{\nu}=258$ (13600), 289 (26400), 314 (14700), 528 nm (77800); UV/Vis ($CHCl_3$/hexane 1:19): 258 (13400), 288 (26300), 313 (14500), 493 (sh, 51100), 524 nm (81100); fluorescence (reference rhodamine 6G; $CHCl_3$): $\phi_F=0.0077$; fluorescence (reference rhodamine 6G; $CHCl_3$/hexane 1:1): $\phi_F=0.054$; fluorescence (reference rhodamine 6G; $CHCl_3$/hexane 1:9): $\phi_F=0.45$; fluorescence (reference rhodamine 6G; $CHCl_3$/hexane 1:19): $\phi_F=0.58$; FT-MALDI-MS (DHB): *m/z*: 364 $[M]^+$; HR-FT-MALDI-MS: *m/z* calcd for $C_{24}H_{20}N_4^+$: 364.1688; found: 364.1683 $[M]^+$.

2-Cyano-3-{[4-(dimethylamino)phenyl]ethynyl}but-2-enedinitrile (19): CuOAc (84 mg, 0.69 mmol) was added to a solution of *N*,*N*-dimethyl-4-ethynylaniline (100 mg, 0.69 mmol) in THF (3 mL). After heating for 20 min to 50°C, the mixture was cooled to RT. A solution of TCNE (71 mg, 0.55 mmol) in THF (2.5 mL) was slowly added. After stirring for 1 h at RT and subsequent CC (CH_2Cl_2), **19** (39 mg, 29%) was obtained as a blue metallic solid. M.p. >164°C (decomp); ^{1}H NMR (300 MHz, $CDCl_3$): $\delta=3.17$ (s, 6H), 6.70 (d, $J=9.0$ Hz, 2H), 7.54 ppm (d, $J=9.0$ Hz, 2H); ^{13}C NMR (75 MHz, $CDCl_3$): $\delta=40.24$, 91.00, 91.06, 104.21, 111.36, 111.40, 111.55, 112.10, 120.52, 125.31, 136.38, 153.41 ppm; IR (KBr): $\tilde{\nu}=$ 3460, 2920, 2168, 1601, 1538, 1475, 1381, 1245, 1197, 1120, 1063, 967, 936, 817, 791 cm^{-1}; UV/Vis ($CHCl_3$): λ (ε)=286 (10700), 341 (sh, 7100), 591 nm (43800); UV/Vis ($CHCl_3$/hexane 1:1): λ (ε)=280 (9900), 291 (9900), 317 (7800), 572 nm (41900); UV/Vis ($CHCl_3$/hexane 1:9): λ (ε)= 274 (10600), 289 (11200), 314 (9100), 325 (sh, 8200), 543 nm (48900); UV/Vis ($CHCl_3$/hexane 1:19): λ (ε)=273 (10400), 288 (11200), 309 (9100), 327 (sh, 8000), 539 nm (52500); fluorescence (reference sulforhodamine 101; $CHCl_3$/hexane 1:19): $\phi_F=0.002$; EI-MS (70 eV): *m/z* (%): 246 (100) $[M]^+$, 230 (10) $[M-\mathrm{H}-\mathrm{Me}]^+$, 221 (11) $[M+\mathrm{H}-\mathrm{CN}]^+$; HR-EI-MS: *m/z* calcd for $C_{15}H_{10}N_4^+$: 246.0905; found: 246.0904 $[M]^+$.

(*Z*)- and (*E*)-2,3-Bis[(triisopropylsilyl)ethynyl]-5-[4-(dimethylamino)phenyl]pent-2-en-4-ynenitrile ((*Z*)-12 and (*E*)-12): $i\mathrm{Pr}_2\mathrm{EtN}$ (50 μL, 0.29 mmol) was added to a solution of **37** (85 mg, 0.24 mmol) and 4-(triisopropylsilyl)but-3-ynenitrile (64 mg, 0.29 mmol) in EtOH (15 mL). After stirring for 5 d at RT in the dark, the solvent was evaporated. Subsequent CC (CH_2Cl_2/hexane 2:1) afforded (*Z*)-**12** (40 mg, 30%) as a red solid and (*E*)-**12** (67 mg, 50%) as a dark orange oil (isolated yield after multiple purifications, since compounds isomerize in hexane).

*Data for (Z)-**12***: M.p. 90°C; ^{1}H NMR (300 MHz, $CDCl_3$): $\delta=1.14$ (m, 42H), 3.04 (s, 6H), 6.63 (d, $J=9.0$ Hz, 2H), 7.37 ppm (d, $J=9.0$ Hz, 2H); ^{13}C NMR (75 MHz, $CDCl_3$): $\delta=11.28$, 11.35, 18.68, 18.75, 40.11, 86.56, 99.76, 101.71, 102.92, 105.65, 105.88, 106.92, 107.47, 111.40, 115.81, 126.01, 133.79, 151.06 ppm; IR (CCl_4): $\tilde{\nu}=2944$, 2927, 2888, 2866, 2181, 2142, 1606, 1526, 1463, 1443, 1367, 1344, 1237, 1194, 1151, 1009, 996, 944, 883 cm^{-1}; UV/Vis ($CHCl_3$): λ (ε)=292 (20300), 338 (14800), 464 nm (24400); FT-MALDI-MS (DCTB): *m/z*: 556 $[M]^+$, 513 $[M-i\mathrm{Pr}]^+$, 471 $[M+\mathrm{H}-2i\mathrm{Pr}]^+$; HR-FT-MALDI-MS: *m/z* calcd for $C_{35}H_{52}N_2Si_2^+$: 556.3669; found: 556.3670 $[M]^+$.

*Data for (E)-**12***: ^{1}H NMR (300 MHz, $CDCl_3$): $\delta=1.12$ (m, 42H), 3.03 (s, 6H), 6.63 (d, $J=8.0$ Hz, 2H), 7.42 ppm (d, $J=8.0$ Hz, 2H); ^{13}C NMR (75 MHz, $CDCl_3$): $\delta=11.33$, 11.70, 18.58, 18.75, 40.12, 86.88, 99.68, 101.82, 102.19, 105.62, 105.72, 107.17, 107.35, 111.49, 116.08, 125.55, 133.95, 151.14 ppm; IR (CCl_4): 2945, 2891, 2866, 2185, 2133, 1605, 1526, 1463, 1444, 1367, 1349, 1250, 1133, 1070, 997, 883 cm^{-1}; UV/Vis ($CHCl_3$): λ (ε)=289 (17100), 328 (12000), 467 nm (25000); FT-MALDI-MS (DCTB): *m/z*: 556 $[M]^+$, 513 $[M-i\mathrm{Pr}]^+$, 471 $[M+\mathrm{H}-2i\mathrm{Pr}]^+$; HR-FT-MALDI-MS: *m/z* calcd for $C_{35}H_{52}N_2Si_2^+$: 556.3669; found: 556.3669 $[M]^+$.

2-(1-{[4-(Dimethylamino)phenyl]ethynyl}-3-(trimethylsilyl)prop-2-ynylidene)malononitrile (15): A mixture of **38** (250 mg, 0.928 mmol), $CH_2(CN)_2$ (107 mg, 1.62 mmol), and Al_2O_3 (activity II-III, 485 mg) in CH_2Cl_2 (2 mL) was heated to reflux for 1 h. The mixture was extracted with CH_2Cl_2 and passed through a plug (CH_2Cl_2). The filtrate was evaporated in vacuo, affording **15** (227 mg, 77%) as a dark metallic solid. M.p. 179°C; ^{1}H NMR (300 MHz, $CDCl_3$): $\delta=0.32$ (s, 9H), 3.09 (s, 6H), 6.65 (d, $J=9.0$ Hz, 2H), 7.51 ppm (d, $J=9.0$ Hz, 2H); ^{13}C NMR (75 MHz, $CDCl_3$): $\delta=-0.66$, 40.08, 88.55, 89.82, 97.83, 105.33, 111.55, 112.86, 113.02, 114.64, 115.53, 134.06, 135.37, 152.28 ppm; IR (neat): $\tilde{\nu}=2961$, 2905, 2225, 2151, 1600, 1531, 1478, 1412, 1380, 1361, 1254, 1240, 1192, 1142, 1132, 1065, 1005, 986, 945, 843, 814, 796, 759, 719 nm; UV/Vis ($CHCl_3$): λ (ε)=293 (26000), 314 (sh, 11400), 326 (sh, 10800), 520 nm (36800); UV/Vis ($CHCl_3$/hexane 1:9): λ (ε)=286 (26700), 312 (10900), 323 (10100), 348 (sh, 4300), 490 nm (37400); UV/Vis (hexane): λ (ε)= 284 (29300), 311 (11900), 323 (10800), 348 (4100), 485 nm (42700); fluorescence (reference rhodamine 6G; $CHCl_3$/hexane 1:9): $\phi_F=0.006$; fluorescence (reference rhodamine 6G; hexane): $\phi_F=0.044$; FT-MALDI-MS (DHB): *m/z*: 317 $[M]^+$; HR-FT-MALDI-MS: *m/z* calcd for $C_{19}H_{19}N_3Si^+$: 317.1348; found: 317.1340 $[M]^+$.

2-(1-{[4-(Dimethylamino)phenyl]ethynyl}-5-(trimethylsilyl)penta-2,4-diynylidene)malononitrile (16): THF/MeOH 1:1 (20 mL) was added to **15** (30 mg, 0.094 mmol). After stirring for 1 h at RT, CH_2Cl_2 (20 mL) and H_2O (20 mL) were added. The aqueous layer was extracted with CH_2Cl_2, and the collected organic layers were washed twice with sat. NaCl solution. After drying with $MgSO_4$ and concentration to ~20 mL, $Me_3SiC{\equiv}CH$ (185 mg, 1.89 mmol) and Hay catalyst (0.18 mL, 0.023 mmol) were added. After stirring for 20 min at RT, the solvent was evaporated. Subsequent CC (CH_2Cl_2) resulted in **16** (7.6 mg, 24%) as a green metallic solid. M.p. 148°C; ^{1}H NMR (300 MHz, $CDCl_3$): $\delta=0.28$ (s, 9H), 3.10 (s, 6H), 6.65 (d, $J=9.2$ Hz, 2H), 7.50 ppm (d, $J=9.2$ Hz, 2H); ^{13}C NMR (75 MHz, $CDCl_3$): $\delta=-0.81$, 40.02, 69.57, 86.12, 89.01, 89.17, 89.95, 102.63, 105.17, 111.71, 112.84, 112.93, 116.54, 132.93, 135.58, 152.58 ppm; IR (neat): $\tilde{\nu}=2923$, 2855, 2162, 2100, 1599, 1532, 1472, 1442, 1394, 1366, 1250, 1183, 1056, 1000, 942, 893, 843, 816, 763 cm^{-1}; UV/Vis ($CHCl_3$): λ (ε)=302 (20900), 320 (21000), 356 (13900), 376 (sh, 10000), 551 nm (32500); FT-MALDI-MS (DHB): *m/z*: 341 $[M]^+$; HR-FT-MALDI-MS: *m/z* calcd for $C_{21}H_{19}N_3Si^+$: 341.1348; found: 341.1340 $[M]^+$.

2-(3-[4-(Dimethylamino)phenyl]-1-{[4-(dimethylamino)phenyl]ethynyl}-prop-2-ynylidene)malononitrile (17): A mixture of **39** (37 mg, 0.12 mmol), $CH_2(CN)_2$ (23 mg, 0.35 mmol), and Al_2O_3 (activity II-III, 103 mg) in CH_2Cl_2 (2 mL) was heated to reflux for 1 h. The mixture was extracted with CH_2Cl_2 and passed through a plug (CH_2Cl_2). The filtrate was evaporated in vacuo, affording **17** (28 mg, 65%) as a green metallic solid. M.p. >240°C (decomp); ^{1}H NMR (300 MHz, $CDCl_3$): $\delta=3.08$ (s, 12H), 6.65 (d, $J=9.0$ Hz, 4H), 7.53 ppm (d, $J=9.0$ Hz, 4H); ^{13}C NMR (75 MHz, $CDCl_3$): $\delta=40.07$, 84.58, 87.58, 105.94, 111.53, 112.52, 114.06, 134.94, 135.03, 151.98 ppm; IR (KBr): $\tilde{\nu}=3422$, 2923, 2853, 2179, 2145,

1601, 1528, 1459, 1441, 1365, 1280, 1234, 1188, 1103, 981, 943, 813 cm^{-1}; UV/Vis ($CHCl_3$): λ (ε) = 296 (25600), 347 (4000), 524 nm (47300); UV/Vis ($CHCl_3$/hexane 1:1): λ (ε) = 293 (25100), 326 (sh, 7300), 345 (sh, 3200), 508 nm (49000); UV/Vis ($CHCl_3$/hexane 1:9): λ (ε) = 287 (25500), 323 (sh, 7300), 339 (sh, 2700), 489 nm (55500); fluorescence (reference rhodamine 6G; $CHCl_3$/hexane 1:9): ϕ_F = 0.012; fluorescence (reference rhodamine 6G; $CHCl_3$/hexane 1:1): ϕ_F = 0.002; FT-MALDI-MS (DHB): *m/z*: 364 $[M]^+$, 387 $[M+Na]^+$; elemental analysis calcd (%) for $C_{24}H_{20}N_4$ (364.45): C 79.10, H 5.53, N 15.37; found: C 79.14, H 5.64, N 15.22.

3,8-Bis{[4-(dimethylamino)phenyl]ethynyl}-2,9-dicyanodeca-2,8-diene-4,6-diynedinitrile (20): MeOH/THF 1:1 (20 mL) was added to **15** (75 mg, 0.24 mmol). After stirring for 30 min at RT, CH_2Cl_2 (20 mL) and H_2O (20 mL) were added. The aqueous layer was extracted with CH_2Cl_2, and the collected organic layers were washed twice with sat. NaCl solution. After drying with $MgSO_4$ and concentration to ~20 mL, Hay catalyst (0.325 mL, 0.042 mmol) was slowly added. After stirring for 30 min, the mixture was subjected to CC (CH_2Cl_2). Recrystallization from CH_2Cl_2/hexane and subsequent CC (CH_2Cl_2) afforded **20** (10.8 mg, 19%) as a black solid. M.p. > 410 °C; ^{1}H NMR (300 MHz, $CDCl_3$): δ = 3.12 (s, 12H), 6.67 (d, *J* = 9.0 Hz, 4H), 7.55 ppm (d, *J* = 9.0 Hz, 4H); ^{13}C NMR (75 MHz, $CDCl_3$): δ = 40.17, 81.24, 85.17, 89.60, 90.41, 105.00, 111.78, 112.60, 112.65, 119.12, 130.99, 135.81, 152.74 ppm; IR (KBr): $\tilde{\nu}$ = 3447, 2920, 2224, 2159, 2142, 1599, 1534, 1472, 1440, 1379, 1361, 1243, 1191, 1131, 1120, 976, 939, 816 cm^{-1}; UV/Vis ($CHCl_3$): λ (ε) = 311 (26300), 403 (16300), 600 nm (30700); FT-MALDI-MS (DHB): *m/z*: 511 $[M+Na]^+$, 489 $[M+H]^+$, 474 $[M+H-Me]^+$; HR-FT-MALDI-MS: *m/z* calcd for $C_{32}H_{20}N_6^+$: 488.1749; 488.1739 $[M]^+$.

3,12-Bis{[4-(dimethylamino)phenyl]ethynyl}-2,13-dicyanotetradeca-2,12-diene-4,6,8,10-tetraynedinitrile (21): THF/MeOH 1:1 (10 mL) was added to **16** (15 mg, 0.044 mmol). After stirring for 30 min at RT, CH_2Cl_2 (20 mL) and H_2O (20 mL) were added. The aqueous layer was extracted with CH_2Cl_2, and the collected organic layers were washed twice with sat. NaCl solution. After drying with $MgSO_4$, the solvent was evaporated in vacuo. The residue was redissolved in THF (5 mL) and $Cu(OAc)_2$ was added. The mixture was stirred for five days at RT. Subsequent CC (CH_2Cl_2) afforded **21** (9.3 mg, 79%) as a black metallic solid. M.p. > 410 °C, but partially polymerized; ^{1}H NMR (300 MHz, $CDCl_3$): δ = 3.10 (s, 12H), 6.67 (d, *J* = 9.2 Hz, 4H), 7.52 ppm (d, *J* = 9.2 Hz, 4H); ^{13}C NMR (75 MHz, $CDCl_3$): δ = 40.09, 65.79, 72.09, 74.07, 87.13, 89.53, 90.83, 105.01, 111.84, 112.67, 112.74, 118.41, 131.07, 135.83, 152.83 ppm; IR (neat): $\tilde{\nu}$ = 2924, 2854, 2140, 1598, 1532, 1465, 1442, 1367, 1252, 1172, 1108, 1044, 997, 942, 817, 788 cm^{-1}; UV/Vis ($CHCl_3$): λ (ε) = 297 (36400), 317 (39600), 332 (34100), 358 (34600), 386 (30100), 419 (25300), 457 (21000), 608 nm (41800); FT-MALDI-MS (DCTB): *m/z*: 536 $[M]^+$; HR-FT-MALDI-MS: *m/z* calcd for $C_{36}H_{20}N_6^+$: 536.1749; found: 536.1749 $[M]^+$.

2-{[4-(Dimethylamino)phenyl]ethynyl}-5-(triisopropylsilyl)-3-[(triisopropylsilyl)ethynyl]pent-2-en-4-ynenitrile (13): *i*Pr_2NH (98 μL, 0.70 mmol), $[PdCl_2(PPh_3)_2]$ (8.2 mg, 0.012 mmol), and CuI (3.3 mg, 0.017 mmol) were added to a degassed solution (Ar) of **40** (105 mg, 0.233 mmol) and *N,N*-dimethyl-4-ethynylaniline (102 mg, 0.702 mmol) in benzene (7 mL). After stirring for 16 h at RT, the solvent was evaporated. Subsequent CC (CH_2Cl_2/hexane 1:1) resulted in **13** (123 mg, 94%) as a red oil that solidified upon standing. M.p. 90 °C; ^{1}H NMR (300 MHz, $CDCl_3$): δ = 1.14 (m, 42H), 3.03 (s, 6H), 6.63 (d, *J* = 9.0 Hz, 2H), 7.36 ppm (d, *J* = 9.0 Hz, 2H); ^{13}C NMR (75 MHz, $CDCl_3$): δ = 11.10, 11.14, 18.49, 18.55, 39.99, 83.52, 102.09, 102.26, 105.11, 105.80, 106.66, 107.51, 107.60, 111.46, 115.34, 120.77, 133.37, 150.95 ppm; IR (neat): $\tilde{\nu}$ = 2943, 2864, 2190, 2140, 1605, 1532, 1459, 1444, 1368, 1343, 1259, 1232, 1194, 1125, 1074, 1013, 1000, 946, 920, 883, 810, 744 cm^{-1}; UV/Vis ($CHCl_3$): λ (ε) = 293 (22900), 324 (18700), 344 (sh, 14300), 470 nm (30100); UV/Vis (hexane): λ (ε) = 284 (21200), 317 (16800), 324 (sh, 16500), 335 (sh, 13200), 435 (sh, 29100), 458 nm (34800); fluorescence (reference anthracene; hexane): ϕ_F = 0.39; FT-MALDI-MS (DHB): *m/z*: 557 $[M+H]^+$, 579 $[M+Na]^+$; HR-FT-MALDI-MS: *m/z* calcd for $C_{35}H_{53}N_2Si_2$: 557.3747; found: 557.3717 $[M+H]^+$; elemental analysis calcd (%) for $C_{35}H_{52}N_2Si_2$ (556.98): C 75.48, H 9.41, N 5.03; found: C 75.04, H 9.42, N 4.95;

(*Z*)- and (*E*)-2-{[4-(Dimethylamino)phenyl]ethynyl}-3-[(triisopropylsilyl)-ethynyl]-5-(trimethylsilyl)pent-2-en-4-ynenitrile ((*Z*)-14 and (*E*)-14): *i*Pr_2NH (58 μL, 0.41 mmol), $[PdCl_2(PPh_3)_2]$ (4.8 mg, 0.0069 mmol), and CuI (2.0 mg, 0.010 mmol) were added to a degassed solution (Ar) of **41** (50 mg, 0.14 mmol) and *N,N*-dimethyl-4-ethynylaniline (40 mg, 0.28 mmol) in benzene (5 mL). After stirring for 13 h, the solvent was evaporated. Subsequent CC (CH_2Cl_2/hexane 1:1) resulted in (*Z*)-**14** (27 mg, 42%) and (*E*)-**14** (38 mg, 58%), both as red oils that solidify upon standing. Each isomer contains ~15% of the other isomer, even after multiple purifications.

*Data for (Z)-**14***: M.p. 82–84 °C; ^{1}H NMR (300 MHz, $CDCl_3$): δ = 0.29 (s, 9H), 1.14 (m, 21H), 3.04 (s, 6H), 6.64 (d, *J* = 9.0 Hz, 2H), 7.37 ppm (d, *J* = 9.0 Hz, 2H); ^{13}C NMR (75 MHz, $CDCl_3$): δ = −0.40, 11.17, 18.54, 40.04, 83.80, 100.04, 101.58, 105.64, 106.15, 107.67, 108.52, 109.02, 111.58, 115.21, 120.69, 133.42, 151.04 ppm; IR (neat): $\tilde{\nu}$ = 2944, 2864, 2186, 2138, 1600, 1533, 1458, 1441, 1374, 1340, 1266, 1250, 1194, 1124, 1071, 1010, 998, 947, 922, 885, 845, 807, 758, 742 cm^{-1}; UV/Vis ($CHCl_3$): λ (ε) = 290 (17900), 325 (15300), 471 nm (25600); FT-MALDI-MS (DHB): *m/z*: 473 $[M+H]^+$, 495 $[M+Na]^+$; elemental analysis calcd (%) for $C_{29}H_{40}N_2Si_2$ (472.82): C 73.67, H 8.53, N 5.92; found: C 73.63, H 8.60, N 5.71.

*Data for (E)-**14***: M.p. 94–97 °C; ^{1}H NMR (300 MHz, $CDCl_3$): δ = 0.27 (s, 9H), 1.14 (m, 21H), 3.03 (s, 6H), 6.62 (d, *J* = 9.0 Hz, 2H), 7.36 ppm (d, *J* = 9.0 Hz, 2H); ^{13}C NMR (75 MHz, $CDCl_3$): δ = −0.39, 11.34, 18.71, 40.10, 83.60, 100.04, 101.80, 105.91, 106.92, 107.51, 107.69, 108.23, 111.41, 115.30, 120.43, 133.30, 150.84 ppm; IR (neat): $\tilde{\nu}$ = 2939, 2863, 2185, 2139, 1602, 1532, 1461, 1444, 1367, 1341, 1264, 1251, 1232, 1194, 1122, 1064, 1011, 998, 944, 922, 884, 845, 809, 757, 742 cm^{-1}; UV/Vis ($CHCl_3$): λ (ε) = 292 (20800), 322 (17500), 470 nm (26600); FT-MALDI-MS (DHB): *m/z*: 473 $[M+H]^+$, 495 $[M+Na]^+$; elemental analysis calcd (%) for $C_{29}H_{40}N_2Si_2$ (472.82): C 73.67, H 8.53, N 5.92; found: C 73.54, H 8.44, N 5.72.

2-Cyano-3-(6-[4-(dimethylamino)phenyl]-4-{[4-(dimethylamino)phenyl]-ethynyl}-3-[(triisopropylsilyl)ethynyl]hex-3-ene-1,5-diynyl)but-2-enedinitrile (22): CuOAc (6.8 mg, 0.055 mmol) was added to a degassed solution of **42** in THF/CH_3CN 6:1 (7 mL). The mixture was heated to 50 °C for 1 h and TCNE (64 mg, 0.050 mmol) subsequently added. After stirring for 2 h 40 min, the mixture was filtered through a plug (CH_2Cl_2). CC (CH_2Cl_2/hexane 2:1) yielded **22** (5.6 mg, 21%) as a green solid. M.p. > 410 °C (decomp); ^{1}H NMR (300 MHz, $CDCl_3$): δ = 1.16 (s, 21H), 3.06 (s, 6H), 3.08 (s, 6H), 6.65 (d, *J* = 9.0 Hz, 2H), 6.67 (d, *J* = 9.0 Hz, 2H), 7.47 (d, *J* = 9.0 Hz, 2H), 7.54 ppm (d, *J* = 9.0 Hz, 2H); ^{13}C NMR (75 MHz, $CDCl_3$): δ = 11.29, 18.72, 40.06, 40.08, 89.95, 90.95, 94.01, 94.16, 100.85, 103.11, 106.12, 107.43, 107.84, 110.26, 110.76, 110.82, 111.34, 111.50, 111.54, 111.67, 119.65, 119.80, 129.59, 134.49, 134.83, 151.51, 151.57 ppm; IR (CCl_4): $\tilde{\nu}$ = 2959, 2926, 2861, 2153, 2127, 1602, 1524, 1445, 1364, 1243, 1188, 1152, 1102, 1022, 1000, 945 cm^{-1}; UV/Vis ($CHCl_3$): λ (ε) = 307 (24600), 372 (sh, 13000), 417 (21900), 484 (sh, 8100), 677 (27700), 734 nm (27600); FT-MALDI-MS (DHB): *m/z*: 620 $[M+H]^+$; HR-FT-MALDI-MS: *m/z* calcd for $C_{40}H_{41}N_5Si^+$: 619.3131; found: 619.3134 $[M]^+$.

2-(1,6-Bis[(triisopropylsilyl)ethynyl]-9-[4-(dimethylamino)phenyl]-7-{[4-(dimethylamino)phenyl]ethynyl}non-6-ene-2,4,8-triynylidene)malononitrile (23): THF/MeOH 1:1 (15 mL), **42** (8.8 mg, 0.017 mmol), and $Cu(OAc)_2$ (16.6 mg, 0.0914 mmol) were added to **6** (9.3 mg, 0.026 mmol). After stirring for 6 h at RT, the mixture was passed through a plug (CH_2Cl_2). Subsequent GPC (CH_2Cl_2) yielded **23** (1.7 mg, 13%) as a green solid. M.p. > 410 °C; ^{1}H NMR (300 MHz, $CDCl_3$): δ = 1.15 (m, 42H), 3.036 (s, 6H), 3.044 (s, 6H), 6.65 (pseudo t, *J* = 9.0 Hz, 4H), 7.43 (d, *J* = 9.0 Hz, 2H), 7.46 ppm (d, *J* = 9.0 Hz, 2H); ^{13}C NMR (75 MHz, $CDCl_3$): δ = 11.18, 11.48, 18.61, 18.83, 40.12, 40.15, 79.49, 80.23, 87.74, 88.05, 93.36, 93.58, 95.57, 99.17, 101.60, 102.33, 105.23, 106.09, 108.06, 108.10, 108.40, 111.39, 111.76, 111.93, 112.10, 115.52, 126.39, 132.89, 133.63, 133.82, 150.78, 150.92 ppm; IR (CCl_4): $\tilde{\nu}$ = 2944, 2926, 2866, 2163, 2140, 1605, 1524, 1463, 1446, 1356, 1262, 1230, 1187, 1168, 1119, 1076, 1018, 998, 948, 883 cm^{-1}; UV/Vis ($CHCl_3$): λ (ε) = 311 (35700), 416 (22400), 434 (sh, 22000), 474 (sh, 18500), 554 (18100), 649 nm (sh, 14100); FT-MALDI-MS (DCTB): *m/z*: 798 $[M]^+$; HR-FT-MALDI-MS: *m/z* calcd for $C_{52}H_{62}N_4Si_2^+$: 798.4513; found: 798.4516 $[M]^+$.

8,13-Bis(3-[(4-(dimethylamino)phenyl]-1-{[4-(dimethylamino)phenyl]-ethynyl}prop-2-ynylidene)-3,18-bis[(triisopropylsilyl)ethynyl]-2,19-dicyanoicosa-2,18-diene-4,6,9,11,14,16-hexaynedinitrile (24): Hay catalyst (40 μl, 0.0052 mmol) was added to **45** (8.1 mg, 0.013 mmol) in CH_2Cl_2 (2 mL). The solution was stirred for 6 h at RT. Subsequent CC (CH_2Cl_2/hexane 5:2) afforded **24** (5.7 mg, 70%) as a black solid. M.p. > 410 °C; ^{1}H NMR (300 MHz, $CDCl_3$): $\delta = 1.17$ (m, 42H), 2.98 (s, 12H), 3.06 (s, 12H), 6.58 (d, $J = 9.0$ Hz, 4H), 6.73 (d, $J = 9.0$ Hz, 4H), 7.44 (d, $J = 9.0$ Hz, 4H), 7.50 ppm (d, $J = 9.0$ Hz, 4H); ^{13}C NMR (125 MHz, CD_2Cl_2): $\delta = 11.51$, 18.69, 40.20, 40.24, 80.49, 81.41, 83.47, 83.89, 88.91, 89.29, 91.86, 92.51, 96.38, 99.51, 105.85, 107.67, 107.68, 108.71, 109.67, 112.08, 112.30, 112.46, 112.55, 116.32, 129.02, 133.03, 134.51, 134.59, 151.90, 152.01 ppm; IR ($CHCl_3$): $\tilde{\nu} = 2958$, 2926, 2872, 2858, 2152, 1601, 1526, 1467, 1459, 1378, 1265, 1116, 1013, 863, 819 cm^{-1}; UV/Vis ($CHCl_3$): λ (ε) = 314 (33800), 435 (sh, 15100), 548 (32400), 707 nm (sh, 14000); FT-MALDI-MS (DCTB): m/z: 1284 $[M+H]^+$, 1307 $[M+H+Na]^+$; HR-FT-MALDI-MS: m/z calcd for $C_{86}H_{82}N_8Si_2^+$: 1282.6201; found: 1282.6211 $[M]^+$.

Acknowledgements

This research was supported by the ETH Research Council, the Fonds der Chemischen Industrie (Germany), and by grants from the SOCRATES/ERASMUS exchange program (R.G.), and the Fulbright program (W.C.P.). We thank Dr. C. Thilgen (ETHZ) for assistance with the nomenclature.

[1] a) H. Hauptmann, *Tetrahedron* **1976**, *32*, 1293–1297; b) Y. Hori, K. Noda, S. Kobayashi, H. Taniguchi, *Tetrahedron Lett.* **1969**, *10*, 3563–3566; c) Y. Rubin, C. B. Knobler, F. Diederich, *Angew. Chem.* **1991**, *103*, 708–710; *Angew. Chem. Int. Ed. Engl.* **1991**, *30*, 698–700; d) H. Hopf, M. Kreutzer, P. G. Jones, *Chem. Ber.* **1991**, *124*, 1471–1475.

[2] a) F. Diederich, L. Gobbi, *Top. Curr. Chem.* **1999**, *201*, 43–79; b) F. Diederich, *Chem. Commun.* **2001**, 219–227.

[3] a) F. Mitzel, C. Boudon, J.-P. Gisselbrecht, P. Seiler, M. Gross, F. Diederich, *Chem. Commun.* **2003**, 1634–1635; b) F. Mitzel, C. Boudon, J.-P. Gisselbrecht, P. Seiler, M. Gross, F. Diederich, *Helv. Chim. Acta* **2004**, *87*, 1130–1157.

[4] a) R. R. Tykwinski, M. Schreiber, R. P. Carlon, F. Diederich, V. Gramlich, *Helv. Chim. Acta* **1996**, *79*, 2249–2281; b) R. R. Tykwinski, M. Schreiber, V. Gramlich, P. Seiler, F. Diederich, *Adv. Mater.* **1996**, *8*, 226–231.

[5] R. Spreiter, C. Bosshard, G. Knöpfle, P. Günter, R. R. Tykwinski, M. Schreiber, F. Diederich, *J. Phys. Chem. B* **1998**, *102*, 29–32.

[6] a) R. R. Tykwinski, U. Gubler, R. E. Martin, F. Diederich, C. Bosshard, P. Günter, *J. Phys. Chem. B* **1998**, *102*, 4451–4465; b) U. Gubler, R. Spreiter, C. Bosshard, P. Günter, R. Tykwinski, F. Diederich, *Appl. Phys. Lett.* **1998**, *73*, 2396–2398; c) U. Gubler, C. Bosshard, *Adv. Polym. Sci.* **2002**, *158*, 123–191.

[7] a) J. S. Miller, A. J. Epstein, *Coord. Chem. Rev.* **2000**, *206*, 651–660; b) D. C. Gordon, L. Deakin, A. M. Arif, J. S. Miller, *J. Am. Chem. Soc.* **2000**, *122*, 290–299; c) A. J. Fatiadi, *Synthesis* **1986**, 249–284; d) A. J. Fatiadi, *Synthesis* **1987**, 749–789; e) T. Michinobu, J. C. May, J. H. Lim, C. Boudon, J.-P. Gisselbrecht, P. Seiler, M. Gross, I. Biaggio, F. Diederich, *Chem. Commun.* **2005**, 737–739.

[8] T. Metler, A. Uchida, S. I. Miller, *Tetrahedron* **1968**, *24*, 4285–4297.

[9] a) H. Hopf, M. Kreutzer, *Angew. Chem.* **1990**, *102*, 425–426; *Angew. Chem. Int. Ed. Engl.* **1990**, *29*, 393–395; b) H. Hopf, M. Kreutzer, P. G. Jones, *Angew. Chem.* **1991**, *103*, 1148–1149; *Angew. Chem. Int. Ed. Engl.* **1991**, *30*, 1127–1128.

[10] L. Y. Ukhin, A. M. Sladkov, Z. I. Orlova, *Bull. Acad. Sci. USSR Div. Chem. Sci. (Engl. Transl.)* **1969**, 637–638.

[11] L. Dulog, B. Körner, J. Heinze, J. Yang, *Liebigs Ann.* **1995**, 1663–1671.

[12] For a preliminary communication on CEEs, see: N. N. P. Moonen, C. Boudon, J.-P. Gisselbrecht, P. Seiler, M. Gross, F. Diederich, *Angew. Chem.* **2002**, *114*, 3170–3173; *Angew. Chem. Int. Ed.* **2002**, *41*, 3044–3047.

[13] For a preliminary communication on donor-substituted CEEs, see: N. N. P. Moonen, R. Gist, C. Boudon, J.-P. Gisselbrecht, P. Seiler, T. Kawai, A. Kishioka, M. Gross, M. Irie, F. Diederich, *Org. Biomol. Chem.* **2003**, *1*, 2032–2034.

[14] F. Meyers, S. R. Marder, B. M. Pierce, J. L. Brédas, *J. Am. Chem. Soc.* **1994**, *116*, 10703–10714.

[15] J. Anthony, A. M. Boldi, Y. Rubin, M. Hobi, V. Gramlich, C. B. Knobler, P. Seiler, F. Diederich, *Helv. Chim. Acta* **1995**, *78*, 13–45.

[16] N. N. P. Moonen, Dissertation ETH No. 15468, Zürich, **2004**.

[17] T. Lange, J.-D. van Loon, R. R. Tykwinski, M. Schreiber, F. Diederich, *Synthesis* **1996**, 537–550.

[18] Z. Wang, Y. Gu, A. J. Zapata, G. B. Hammond, *J. Fluorine Chem.* **2001**, *107*, 127–132.

[19] J. M. Schwab, C.-K. Ho, W.-B. Li, C. A. Townsend, G. M. Salituro, *J. Am. Chem. Soc.* **1986**, *108*, 5309–5316.

[20] F. Texier-Boullet, A. Foucaud, *Tetrahedron Lett.* **1982**, *23*, 4927–4928.

[21] E. Kloster-Jensen, *Acta Chem. Scand.* **1963**, *17*, 1866–1874.

[22] J. A. Marsden, M. M. Haley, *Metal-Catalyzed Cross-Coupling Reactions*, *Vol. I*, 2nd ed., (Eds.: A. de Meijere, F. Diederich), Wiley-VCH, Weinheim, **2004**, pp. 317–394.

[23] R. Faust, C. Weber, V. Fiandanese, G. Marchese, A. Punzi, *Tetrahedron* **1997**, *53*, 14655–14670.

[24] A. S. Hay, *J. Org. Chem.* **1962**, *27*, 3320–3321.

[25] P. Siemsen, R. C. Livingston, F. Diederich, *Angew. Chem.* **2000**, *112*, 2740–2767; *Angew. Chem. Int. Ed.* **2000**, *39*, 2632–2657.

[26] G. Eglinton, A. R. Galbraith, *Chem. Ind. (London)* **1956**, 737–738.

[27] K. A. Leonard, M. I. Nelen, T. P. Simard, S. R. Davies, S. O. Gollnick, A. R. Oseroff, S. L. Gibson, R. Hilf, L. B. Chen, M. R. Detty, *J. Med. Chem.* **1999**, *42*, 3953–3964.

[28] K. A. Leonard, M. I. Nelen, L. T. Anderson, S. L. Gibson, R. Hilf, M. R. Detty, *J. Med. Chem.* **1999**, *42*, 3942–3952.

[29] A. Auffrant, F. Diederich, C. Boudon, J.-P. Gisselbrecht, M. Gross, *Helv. Chim. Acta* **2004**, *87*, 3085–3105.

[30] B. Iorga, L. Ricard, P. Savignac, *J. Chem. Soc. Perkin Trans. 1* **2000**, 3311–3316.

[31] R. R. Tykwinski, A. Hilger, F. Diederich, H. P. Lüthi, P. Seiler, V. Gramlich, J.-P. Gisselbrecht, C. Boudon, M. Gross, *Helv. Chim. Acta* **2000**, *83*, 1484–1508.

[32] E. Breitmaier, *Structure Elucidation by NMR in Organic Chemistry: A Practical Guide*, 3rd ed., Wiley, Chichester, **2002**.

[33] M. Barfield, T. Gotoh, H. K. Hall Jr., *Magn. Reson. Chem.* **1985**, *23*, 705–709.

[34] a) C. Dehu, F. Meyers, J. L. Brédas, *J. Am. Chem. Soc.* **1993**, *115*, 6198–6206; b) A. Hilger, J.-P. Gisselbrecht, R. R. Tykwinski, C. Boudon, M. Schreiber, R. E. Martin, H. P. Lüthi, M. Gross, F. Diederich, *J. Am. Chem. Soc.* **1997**, *119*, 2069–2078.

[35] To save calculation time, the silyl protecting groups were replaced by hydrogens, which has been proven a valid simplification: A. Hilger, Dissertation ETH No. 12928, Zürich, **1998**. All calculations were carried out within the Gaussian 98 program: M. J. Frisch, G. W. Trucks, H. B. Schlegel, G. E. Scuseria, M. A. Robb, J. R. Cheeseman, V. G. Zakrzewski, J. A. Montgomery Jr., R. E. Stratmann, J. C. Burant, S. Dapprich, J. M. Millam, A. D. Daniels, K. N. Kudin, M. C. Strain, O. Farkas, J. Tomasi, V. Barone, M. Cossi, R. Cammi, B. Mennucci, C. C. Pomelli, C. Adamo, S. Clifford, J. W. Ochterski, G. A. Petersson, P. Y. Ayala, Q. Cui, K. Morokuma, D. K. Malick, A. D. Rabuck, K. Raghavachari, J. B. Foresman, J. Cioslowski, J. V. Ortiz, B. B. Stefanov, G. Liu, A. Liashenko, P. Piskorz, I. Komaromi, R. Gomperts, R. L. Martin, D. J. Fox, T. Keith, M. A. Al-Laham, C. Y. Peng, A. Nanayakkara, C. Gonzalez, M. Challacombe, P. M. W. Gill, B. Johnson, W. Chen, M. W. Wong, J. L. Andres, C. Gonzalez, M. Head-Gordon, E. S. Replogle, J. A. Pople, Gaussian 98, Revision A.7, Gaussian Inc., Pittsburgh, PA, **1998**.

[36] C. Boudon, J.-P. Gisselbrecht, M. Gross, J. Anthony, A. M. Boldi, R. Faust, T. Lange, D. Philp, J.-D. Van Loon, F. Diederich, *J. Electroanal. Chem.* **1995**, *394*, 187–197.

[37] C. Diaz, A. Arancibia, *Polyhedron* **2000**, *19*, 137–145.
[38] J. E. Mulvaney, R. J. Cramer, H. K. Hall Jr., *J. Polym. Sci. Polym. Chem. Ed.* **1983**, *21*, 309–314.
[39] a) D. W. Rogers, N. Matsunaga, A. A. Zavitsas, F. J. McLafferty, J. F. Liebman, *Org. Lett.* **2003**, *5*, 2373–2375; b) D. W. Rogers, N. Matsunaga, F. J. McLafferty, A. A. Zavitsas, J. F. Liebman, *J. Org. Chem.* **2004**, *69*, 7143–7147; c) P. D. Jarowski, M. D. Wodrich, C. S. Wannere, P. v. R. Schleyer, K. N. Houk, *J. Am. Chem. Soc.* **2004**, *126*, 15036–15037; d) E. K. Wilson, *Chem. Eng. News* **2004**, *82* (NO. 51, December 20), 48.
[40] J.-P. Gisselbrecht, N. N. P. Moonen, C. Boudon, M. B. Nielsen, F. Diederich, M. Gross, *Eur. J. Org. Chem.* **2004**, 2959–2972.
[41] a) N. N. P. Moonen, F. Diederich, *Org. Biomol. Chem.* **2004**, *2*, 2263–2266; b) for a study on the influence of donor and acceptor substitution on the frontier orbitals of cruciform π systems, see: J. N. Wilson, M. Josowicz, Y. Q. Wang, U. H. F. Bunz, *Chem. Commun.* **2003**, 2962–2963.
[42] M. B. Nielsen, M. Schreiber, Y. G. Baek, P. Seiler, S. Lecomte, C. Boudon, R. R. Tykwinski, J.-P. Gisselbrecht, V. Gramlich, P. J. Skinner, C. Bosshard, P. Günter, M. Gross, F. Diederich, *Chem. Eur. J.* **2001**, *7*, 3263–3280.
[43] Z. Rappoport, C. Rav-Acha, *Tetrahedron Lett.* **1984**, *25*, 117–120.
[44] R. F. Kubin, A. N. Fletcher, *J. Lumin.* **1982**, *27*, 455–462.
[45] G. G. Guilbault, *Practical Fluorescence*, Marcel Dekker, New York, **1990**.
[46] http://www.probes.com/handbook/tables/0375.html.
[47] a) P. Suppan, N. Ghoneim, *Solvatochromism*, The Royal Society of Chemistry, Cambridge, **1997**; b) P. Suppan, *J. Photochem. Photobiol. A* **1990**, *50*, 293–330.
[48] E. U. Condon, *Phys. Rev.* **1928**, *32*, 858–872.
[49] a) W. Liptay, R. Wortmann, H. Schaffrin, O. Burkhard, W. Reitinger, N. Detzer, *Chem. Phys.* **1988**, *120*, 429–438; b) H. B. Lueck, J. L. McHale, W. D. Edwards, *J. Am. Chem. Soc.* **1992**, *114*, 2342–2348; c) D. F. Duxbury, *Chem. Rev.* **1993**, *93*, 381–433.
[50] a) E. M. Kober, B. P. Sullivan, T. J. Meyer, *Inorg. Chem.* **1984**, *23*, 2098–2104; b) L. F. Cooley, P. Bergquist, D. F. Kelley, *J. Am. Chem. Soc.* **1990**, *112*, 2612–2617; c) G. Verbeek, S. Depaemelaere, M. van der Auweraer, F. C. De Schryver, A. Vaes, D. Terrell, S. De Meutter, *Chem. Phys.* **1993**, *176*, 195–213; d) W. Verbouwe, M. van der Auweraer, F. C. De Schryver, J. J. Piet, J. M. Warman, *J. Am. Chem. Soc.* **1998**, *120*, 1319–1324.
[51] a) N. Ghoneim, P. Suppan, *Spectrochim. Acta Part A* **1995**, *51*, 1043–1050; b) B. Strehmel, A. M. Sarker, H. Detert, *ChemPhysChem* **2003**, *4*, 249–259.
[52] M. Sheik-Bahae, A. A. Said, T.-H. Wei, D. J. Hagan, E. W. Van Stryland, *IEEE J. Quantum Electron.* **1990**, *26*, 760–769.
[53] a) O.-K. Kim, K.-S. Lee, H. Y. Woo, K.-S. Kim, G. S. He, J. Swiatkiewicz, P. N. Prasad, *Chem. Mater.* **2000**, *12*, 284–286; b) T. D. Krauss, F. W. Wise, *Appl. Phys. Lett.* **1994**, *65*, 1739–1741; c) M. Yin, H. P. Li, S. H. Tang, W. Ji, *Appl. Phys. B* **2000**, *70*, 587–591.
[54] a) H. Meier, B. Mühling, H. Kolshorn, *Eur. J. Org. Chem.* **2004**, 1033–1042; b) H. Meier, J. Gerold, H. Kolshorn, B. Mühling, *Chem. Eur. J.* **2004**, *10*, 360–370.

Received: January 25, 2005
Published online: March 30, 2005

